Coadapted genomes and selection on hybrids: Fisher's geometric model explains a variety of empirical patterns

Alexis Simon[1,2,*], Nicolas Bierne[1], and John J. Welch[2]

1. Institut des Sciences de l'Évolution UMR5554, Université de Montpellier, CNRS-IRD-EPHE-UM, France.
2. Department of Genetics, University of Cambridge, Downing St. Cambridge, CB23EH, UK.

* Author for correspondence: alexis.simon@umontpellier.fr

Abstract

Fitness landscape models play an important role in our understanding of speciation, hybridization and admixture. The simplest modeling approaches are best-suited to particular kinds of hybridization: either crosses between closely-related inbred lines, where hybrids are often fitter than their parents, or crosses between effectively isolated species, where breakdown involves discrete incompatibilities of large effect. We study a fitness landscape based on Fisher's geometric model, and show that it naturally interpolates between these two approaches, while explaining surprising empirical patterns that have been observed in both regimes. The model also yields new predictions, which can be tested with genomic data, and without needing to identify individual loci with anomalous effects. We test these predictions with data from *Mytilus* mussels, and published data from plants (*Zea*, *Populus* and *Senecio*) and animals (*Mus*, *Teleogryllus* and *Drosophila*), and the predictions are generally supported. Fisher's geometric model should be particularly useful for studying hybridization in an intermediate regime, where hybrid fitness might be influenced by allelic coadaptation and maladaptation in the parental lines, and where epistatic interactions might involve many loci of moderate effect.

Keywords

Speciation genetics, heterozygosity, Dobzhansky-Muller incompatibilities, sterility, inbreeding, Haldane's Rule.

1 Introduction

Hybridization and admixture involve testing alleles in alternative genetic backgrounds. Most classical studies of hybridization can be placed into one of two classes. The first, involves crosses between closely-related inbred lines, where there is no coadaptation between the deleterious alleles that differentiate the parental backgrounds, such that most hybrids are fitter than their parents. Wright's single-locus theory of inbreeding was developed to interpret data of this kind (Crow 1952; Hallauer et al. 2010; Wright 1922, 1977). The second, involves crosses between effectively isolated species, where viable and fertile hybrids are very rare. Data of this kind are often analyzed by focusing on a small number of "speciation genes", and interpreted using models of genetic incompatibilities (Coyne and Orr 1989; Dobzhansky 1937; Gavrilets 2004; Kalirad and Azevedo 2017; Orr 1995; Welch 2004).

The differences between these types of hybridization are clear, but it is equally clear that they are extremes of a continuum. Furthermore, the intermediate stages of this continuum are of particular interest, including, as they do, incipient speciation, and occasional introgression between partially-isolated populations (Duranton et al. 2017; Fraïsse et al. 2016a; Mendez et al. 2012; Waser 1993). However, it can be difficult to model natural selection in this intermediate regime, not least because models require a large number of parameters when they include epistatic effects between many loci. The empirical study of hybrid genotypes in this regime is also difficult. The analysis of lab crosses often focuses on segregation distortions of large effect, and pairwise incompatibilities (Abbott et al. 2013; Coyne and Orr 2004). This QTL-mapping framework can miss small effect mutations (Noor et al. 2001; Rockman 2012), which are difficult to identify individually, but whose cumulative effect can be substantial (Boyle et al. 2017).

One promising approach is to use Fisher's geometric model, which assigns fitness values to genotypes using a model of optimizing selection on quantitative traits (Fisher 1930; G. Martin and Lenormand 2006; Orr 1998; Welch and Waxman 2003). The tools of quantitative genetics have often been used to study hybridization (e.g. Demuth and Wade 2005; Fitzpatrick 2008; Lynch 1991; Melchinger 1987), but Fisher's model is fully additive at the level of phenotype, and the "traits" need not correspond in any simple way to standard quantitative traits (G. Martin 2014; Schiffman and Ralph 2017). Instead, the goal is to generate a rugged fitness landscape, which includes a wide variety of mutational effect sizes and epistatic interactions, with a minimum of free parameters (Barton 2017; Hwang et al. 2017).

Here, we build on previous studies (Barton 2001; Chevin et al. 2014; Fraïsse et al. 2016b; Schiffman and Ralph 2017), and use Fisher's geometric model to study hybridization. We develop a simple random-walk approximation, and show that it can naturally interpolate between previous modeling approaches, which are appropriate for the two extreme types of hybridization. We then show how the model can account for surprising empirical patterns that have been observed in both regimes (Moehring 2011; Moran et al. 2017; Wright 1977). Finally, we show that the model yields several novel predictions, and test these predictions with a wide range of new and existing data sets (Table 1).

2 Models and Results

2.1 The models

2.1.1 Notation and basics

We will consider hybrids between two diploid populations, labeled P1 and P2, each of which is genetically uniform, but which differ from each other by d substitutions. The populations could generate 3^d distinct hybrid genotypes, and each might have a different level of fitness, but we are most interested in systematic differences between different types of hybrid (e.g., high versus low heterozygosity, males versus females, F1 versus F2 etc.). As such, following Turelli and Orr (2000), we describe hybrids using a "breakdown score", S, which is larger for hybrids that are less fit. The relationship between S and fitness, w, might take a form such as

$$\ln w \propto -S^{\beta/2} \tag{1}$$

in which case, the parameter β adjusts the overall level of fitness dominance and epistasis, and can vary independently of other results (Fraïsse et al. 2016b; Hinze and Lamkey 2003; Tenaillon et al. 2007; see also Discussion). We now define the key quantity f, as the expected value of S for a particular class of hybrid, scaled by the expected value for the worst possible class.

$$f \equiv \frac{E\left(S\right)}{E\left(S_{+}\right)} \tag{2}$$

Here, $E\left(S_{+}\right)$, is the expected breakdown score for the class of hybrid with the lowest expected fitness. Therefore, f can vary between zero, for the best possible class of hybrid, and one, for the worst possible class.

To define classes of hybrid, we also follow Turelli and Orr (2000). We pay particular attention to inter-population heterozygosity, and define p_{12} as the proportion of the divergent sites that carry one allele from each of the parental types. We also define p_1 and p_2 as the proportion of divergent sites that carry only alleles originating from P1 or P2 respectively. Since $p_1 + p_2 + p_{12} = 1$, it is convenient to introduce the hybrid index, h, which we define as the total proportion of alleles that originates from P2 (e.g. Fitzpatrick 2012).

$$h \equiv p_2 + \frac{1}{2}p_{12} \tag{3}$$

Each individual genotype can now be described via its heterozygosity, p_{12}, and its hybrid index, h. Results below will mainly concern the dependency of f on p_{12} and h.

2.1.2 Fisher's geometric model

Fisher's model is defined by n quantitative traits under optimizing selection (Fisher 1930). If the selection function is multivariate normal, including correlated selection, then we can rotate the axes

and scale the trait values, to specify n new traits which are under independent selection of different strengths (G. Martin 2014; G. Martin and Lenormand 2006; Waxman and Welch 2005). An example with $n = 2$ is shown in Figure 1. We now define the breakdown score of a phenotype as

$$S \equiv \sum_{i=1}^{n} \lambda_i z_i^2 \tag{4}$$

where, for trait i, z_i is its deviation from the optimum and λ_i is the strength of selection. By assumption, all mutational changes act additively on each trait, but their effects on breakdown can vary with the phenotype of the individual in which they appear, and this yields fitness epistasis. To specify the breakdown for each hybrid genotype, we would need to know the sizes and directions of all of the mutations that differentiate P1 and P2. However, a useful approximation is to treat the recombinant hybrid genotypes as if they lie along random walks in phenotypic space, where each fixed mutation contributes an expected v_i to the variance of the random walk on trait i. In this case, the worst possible class of hybrid will lie at the end of an unconstrained random walk away from the optimum, with no tendency for coadaptation among the changes. The walk can involve a maximum of d substitutions, and so we have

$$E\left(S_{\dagger}\right) \equiv d \sum_{i=1}^{n} \lambda_i v_i \tag{5}$$

Most hybrid genotypes will have higher fitness than this, because they contain combinations of alleles that are coadapted, as a result of past natural selection in their original backgrounds. To find the value of f (eq. 2) that applies to these genotypes, let us first assume that P1 and P2 are sufficiently well adapted, compared to the worst class of hybrid, to be treated as optimal. In this case, we fix f at zero for both parental types: $f_{\mathrm{P1}} = f_{\mathrm{P2}} = 0$. This implies that the midparental phenotype will also be optimal, and given the assumption of additivity, this midparent will be associated with the global heterozygote. We can now model the hybrid phenotypes as lying on a tethered random walk, or Brownian bridge, with these three optimal genotypes as fixed points; f is the variance associated with this Brownian bridge. In Appendix 1, we show that the result required is

$$f = p_{12}(1 - p_{12}) + 4p_1p_2 \tag{6}$$

$$= 4h(1 - h) - p_{12} \tag{7}$$

The fitness surface that is implied by eq. 7 is shown in Figure 2a. It should be noted that this prediction does not depend on any of the model parameters. For example, the number of traits, n, could affect the accuracy of the random-walk approximation (since S will tend to approach normality as n increases). But n does not appear in eq. 7, which depends on p_{12} and h alone.

It is also possible to relax the assumption that the parents are optimally fit. In Appendix 1, we show that a simple and useful expression arises when the midparent is optimal, but the parents are

suboptimal. This implies that both parents are equally maladapted: $f_{P1} = f_{P2} \equiv f_P$, and we find that

$$f = p_{12}(1 - p_{12}) + 4p_1p_2 + (p_1 - p_2)^2 f_P \tag{8}$$

$$= f_P + (1 - f_P)\, 4h(1 - h) - p_{12} \tag{9}$$

Fitness surfaces with varying levels of parental maladaptation are illustrated in Supplementary Figure S1. As expected, eq. 9 reduces to eq. 7 when $f_P = 0$, while in the other extreme case, when $f_P = 1$ we find,

$$f = 1 - p_{12}, \qquad f_P = 1 \tag{10}$$

In this case, when parental fitness is no higher than the expected fitness of a random assembly of their alleles (eq. 2), then the breakdown is proportional to the total homozygosity (eq. 10). This result agrees with Wright's (1922) single-locus theory of inbreeding, which was developed to analyze crosses between closely-related inbred lines (see also eq. 18 below). This agreement makes intuitive sense: when $f_P = 1$, all of the divergence between P1 and P2 must comprise deleterious mutations with no coadaptation. In its general form (eq. 9), Fisher's model shows how coadaptation between the parental alleles affects selection in the hybrids.

2.1.3 A general model of incompatibilities

The previous section showed that Wright's theory of inbreeding appears as a special case of Fisher's geometric model, when $f_P = 1$. In this section, we show that the other extreme case, with $f_P = 0$, can also be derived via an alternative route, using a widely-used model from speciation genetics. We show that eq. 7 can be obtained from a model of genetic incompatibilities, each involving alleles at a small number of loci (Fraïsse et al. 2016b; Gavrilets 2004; Orr 1995; Turelli and Orr 2000; Welch 2004). The aim of this section is solely to compare the two modeling approaches. Empirical tests of eq. 9 follow in subsequent sections.

Following Orr (1995), let us assume that certain combinations of alleles, at $\ell \leq d$ of the divergent loci, can be intrinsically incompatible, while all other combinations confer high fitness. By assumption, the pure species genotypes, and their ancestral states, must be fit, but all other combinations have a fixed probability ε_ℓ of being incompatible. Under this model, the expected breakdown score for the worst class of hybrid is proportional to the expected number of incompatibilities, and this was calculated by Welch (2004, eqs. 1-2):

$$E\left(S_+\right)_I \propto \varepsilon_\ell \binom{d}{\ell} \left(2^\ell - \ell - 1\right) \tag{11}$$

Here, and below, we use the subscript I to indicate a model of incompatibilities. To derive f_I (eq. 2), we note that hybrids will have higher fitness when some of the incompatibilities are absent from their genomes (Turelli and Orr 2000). The probability that an incompatibility is present depends on how many of the ℓ loci are heterozygous. For a genotype comprising i loci that are homozygous for the P1

allele, j loci homozygous for the P2 allele, and k loci that are heterozygous, the probability required is:

$$\pi_{ijk} = \frac{2^k - 0^i - 0^j}{2^\ell - 2} \tag{12}$$

which is the proportion of the possible combinations of heterospecific alleles that are present in an "ijk" genotype. Incompatibilities may also have reduced effects due to recessivity, when their negative effects are masked by the presence of alternative, compatible alleles (Turelli and Orr 2000). To model this, we introduce the free parameter s_{ijk}, which is the expected increase in breakdown when an incompatibility appears in an ijk genotype. Finally, in a hybrid genome characterized by p_1, p_2 and p_{12}, the trinomial expansion of $(p_1 + p_2 + p_{12})^\ell$, tells us how many ℓ-locus genotypes of each type it is expected to contain. Putting these together, we have

$$f_I = \sum_{i+j+k=\ell} \binom{\ell}{i,j,k} p_1^i p_2^j p_{12}^k \pi_{ijk} s_{ijk} \tag{13}$$

Equations 12-13 extend results with $\ell = 2$ and $\ell = 3$ from Turelli and Orr (2000), and represent a general model of breakdown caused by incompatibilities. A notable feature of these equations is their large number of free parameters. Even with symmetry between P1 and P2 (such that $s_{ijk} = s_{jik}$), we will still require a total of $\lfloor \ell(1 + \ell/4) \rfloor$ different s_{ijk} values to specify the model (i.e., three extra parameters for two-locus incompatibilities, five parameters for three-locus incompatibilities etc.). There is good empirical evidence for, at least, two- three- and four-locus incompatibilities (Fraïsse et al. 2014), and so the full model would depend on at least 17 free parameters. By contrast, eq. 6, from Fisher's geometric model, has no free parameters. The incompatibility-based model is therefore much more flexible, but also much more difficult to explore.

Because of this flexibility, however, it is also possible to find a set of s_{ijk} values that yield exactly the same dependencies as Fisher's model. To do this, we set $f_I = f$, using eqs. 6 and 13, and then solve for the s_{ijk}. After some algebra, we find

$$s_{ijk} = \frac{(i+j)\ell - (i-j)^2}{\ell(\ell-1)\pi_{ijk}} \tag{14}$$

Equation 14 looks unwieldy, and it was derived solely to make the models agree. Nevertheless, in Appendix 2 and Supplementary Figure S2, we show that it embodies biologically plausible assumptions about incompatibilities, namely (i) partial recessivity, and (ii) increased levels of breakdown when incompatibilities are present with homozygous alleles from both parental lines. We further show that these s_{ijk} fall within the relatively narrow range of values that are required if the model is to yield a range of well-established empirical patterns (see also Turelli and Orr 2000). As such, when parental lines are well adapted compared to the worst possible class of hybrid ($f_P = 0$), the key predictions of Fisher's geometric model can also be derived from a general model of incompatibilities.

2.2 Testing the predictions with biparental inheritance

2.2.1 Fitness differences between crosses

The simplest predictions from eq. 9 assume standard biparental inheritance at all loci. In this case, the standard cross types can be easily located on the fitness landscape shown in Figure 2a (Fitzpatrick 2012). With biparental inheritance, hybrids from the initial F1 cross (P1 $\times$ P2) will be heterozygous at all divergent loci ($p_{12} = 1$ and $h = \frac{1}{2}$); as such, eq. 9 predicts no breakdown for these F1.

$$f_{\mathrm{F1}} = 0 \tag{15}$$

If the parental types are maladapted, then eq. 15 implies that $f_{\mathrm{P}} > f_{\mathrm{F1}}$, and so there will be F1 hybrid vigor. Hybrid vigor can also appear at later crosses, but only when the parents are very maladapted. To see this, we can rearrange eq. 9 to provide a general condition for hybrid vigor:

$$f_{\mathrm{P}} > 1 - \frac{p_{12}}{4h(1-h)} \tag{16}$$

This condition will be much harder to satisfy for crosses beyond the F1. For example, in the first backcross (F1 $\times$ P1), all heterospecific alleles are heterozygous, and the expected heterozygosity is 50%: $h = \frac{p_{12}}{2}$, $E(p_{12}) = \frac{1}{2}$ (Fitzpatrick 2012). As such, eq. 16 predicts hybrid vigor only when $f_{\mathrm{P}} > (1 - p_{12})/(2 - p_{12}) \approx \frac{1}{3}$. Conditions for hybrid vigor are even more stringent in the F2 (F1 $\times$ F1), when the expected hybrid index and heterozygosity are both 50%: $E(h) = E(p_{12}) = \frac{1}{2}$. With these values, F2 hybrid vigor is predicted only when $f_{\mathrm{P}} > \frac{1}{2}$. Taken together, these results predict that F1 vigor will be common, while hybrid breakdown will often appear in later crosses. This pattern has widespread empirical support (see references in Table A1 of Fraïsse et al. 2016b).

The model also makes quantitative predictions about the relative fitness of different crosses. Extensive data to test these predictions are available for *Zea mays*; these involve crosses of closely related and highly inbred lines, which do show hybrid vigor in the F2 and later crosses (Hallauer et al. 2010; Hinze and Lamkey 2003; Melchinger 1987; Neal 1935; Wright 1977). To analyze these data, a widely-used proxy for fitness is the excess yield of a cross, scaled by the excess yield of the F1. From eqs. 1-2, the relevant quantity is approximately equal to

$$\frac{w - w_{\mathrm{P}}}{w_{\mathrm{F1}} - w_{\mathrm{P}}} \approx 1 - (f/f_{\mathrm{P}})^{\beta/2} \tag{17}$$

$$= 1 - p_{12}, \qquad f_{\mathrm{P}} = 1, \beta = 2 \tag{18}$$

where w and f are the fitness and relative breakdown score for the hybrid of interest. For later crosses, these values will vary between individuals within a cross, due to segregation and recombination, but in this section we ignore this variation, and assume that p_{12} and h take their expected values for a given cross type. A fuller treatment is outlined in Appendix 3.

Equation 18 confirms that Fisher's model reduces to Wright's (1922) single-locus predictions for inbreeding, but only when all divergence is deleterious ($f_{\mathrm{P}} = 1$), and increases in breakdown score

act independently on log fitness ($\beta = 2$). These single-locus predictions have strong support in *Zea mays* (Hallauer et al. 2010; Hinze and Lamkey 2003; Melchinger 1987; Neal 1935; Wright 1977). For example, as shown in Figure 3a, the excess yield of the F2 is often around 50%, equal to its expected homozygosity (Hallauer et al. 2010; Wright 1977). It is also notable that the two outlying points (from Shehata and Dhawan 1975), are variety crosses, and not inbred lines in the strict sense.

Despite this predictive success, Wright (1977) noted a pattern that single-locus theory could not explain. In Wright's words: "the most consistent deviation from expectation [...] is the low yield of F2 in comparison with the first backcrosses" (Wright 1977, p. 39). Because $E(p_{12}) = \frac{1}{2}$ for both crosses, this difference must involve fitness epistasis. In fact, the pattern is predicted by Fisher's model, when there is a small amount of coadaptation between the fixed alleles, such that $0.5 < f_P < 1$ (see Supplementary Figure S1 for fitness surfaces of this type). To show this, Figure 3b plots the four relevant data sets collated by Wright, and compares the results to predictions from eq. 17 with $f_P = 0.75$. The model predicts the roughly linear increase in vigor with mean heterozygosity, as with single locus theory, but also predicts the consistent difference in vigor between the backcross and F2.

2.2.2 Selection on heterozygosity within crosses

In the previous section, we ignored between-individual variation in heterozygosity within a given cross type. In this section, we show how natural selection is predicted to act on this heterozygosity.

First, let us consider the F2. In this case, we have $4h(1-h) \approx 1$ with relatively little variation between individuals (see Appendix 3 for details). Therefore, eq. 9 is well approximated by

$$f_{F2} \approx 1 - p_{12} \tag{19}$$

and so Wright's result (eq. 10), applies in the F2, regardless of parental adaptedness. The prediction is that p_{12} will be under directional selection in the F2, favoring individuals with higher heterozygosity.

Now let us consider a backcross: F1 $\times$ P1. In this case, we have $p_2 = 0$, and so eq. 8 becomes

$$f_{BC} = (1 - f_P)\, p_{12}\, (1 - p_{12}) + f_P\, (1 - p_{12}) \tag{20}$$

$$= p_{12}(1 - p_{12}), \qquad f_P = 0 \tag{21}$$

So selection in backcrosses varies with parental maladaptation. When $f_P > 0.5$ there is directional selection for higher heterozygosity, as in the F2. But when f_P is smaller, intermediate values of p_{12} yield the lowest expected fitness; when $f_P = 0$, heterozygosity is under symmetrical disruptive selection, favoring heterozygosities that are either higher or lower than $p_{12} = 0.5$ (eq. 21). These contrasting predictions are illustrated in Figure 2b (see also Supplementary Figure S1).

To test these predictions, we used a new data set of genetic data from hybrids of the mussel species: *Mytilus edulis* and *Mytilus galloprovincialis* (Bierne et al. 2006, 2002). These species fall at the high end of the continuum of divergence during which introgression persists among incipient species (Roux et al. 2016). We used experimentally bred F2 and first backcrosses, with selection imposed implicitly, by

the method of fertilization, and by our genotyping only individuals who survived to reproductive age (Bierne et al. 2006, 2002; see Methods and Supplementary Figure S3 for full details).

To estimate heterozygosity in each hybrid individual, we used the 43 markers that were heterozygous in all of the F1 hybrids used to make the subsequent crosses (see Supplementary Figure S3). We then asked whether the distribution of p_{12} values in recombinant hybrids was symmetrically distributed around its Mendelian expectation of $p_{12} = 0.5$, or whether it was upwardly biased, as would be expected if directional selection were acting on heterozygosity. As shown in the first column of Table 2, Wilcoxon tests found that heterozygosities in surviving hybrids were significantly higher than expected, in both the F2 and backcross. These results may have been biased by the inclusion of individuals with missing data, because they showed higher heterozygosity (see Supplementary Table S1). We therefore repeated the test with these individuals excluded. As shown in the second column of Table 2, results were little changed, although the bias towards high heterozygosities was now weaker in the backcross.

Interpreting these results is complicated by the ongoing gene flow between *M. edulis* and *M. galloprovincialis* in nature (Bierne et al. 2002; Fraïsse et al. 2016a). To test for this, we genotyped 129 pure-species individuals, and repeated our analyses with a subset of 33 markers that were strongly differentiated between the pure species (see Methods, Supplementary Figure S3 and Supplementary Table S4 for details). With these markers, there was evidence of elevated heterozygosity in the F2, but not the backcross (Table 2 third column). We also noticed that many of our backcross hybrids, though backcrossed to *M. galloprovincialis*, carried homozygous alleles that were typical of *M. edulis*. We therefore repeated our analysis after excluding these "F2-like" backcrosses. Results, shown in the fourth column of Table 2, showed that the reduced BC data set showed no tendency for elevated heterozygosity. However, the bias towards higher heterozygosities remained in the F2, even when we subsampled to equalize the sample sizes.

Despite the problems of interpretation due to introgression and shared variants, the results support the prediction of eqs. 19-21: that directional selection on heterozygosity should act in the F2, but weakly or not at all in the backcross.

2.3 Predictions of Fisher's geometric model with sex-specific inheritance

2.3.1 Additional notation and basics

Results above assumed exclusively biparental inheritance. But the predictions of Fisher's model are easily extended to include heteromorphic sex chromosomes, or loci with strictly uniparental inheritance, such as organelles or imprinted loci (Coyne and Orr 1989; Fraïsse et al. 2016b; Turelli and Moyle 2007; Turelli and Orr 2000). In these cases, p_{12}, p_1 and p_2 are weighted sums of contributions from different types of locus. For example, with an X chromosome and autosomes, we have

$$\begin{aligned} p_{12} &= g_X\, p_{12,X} + g_A\, p_{12,A} \\ p_1 &= g_X\, p_{1,X} + g_A\, p_{1,A} \\ p_2 &= g_X\, p_{2,X} + g_A\, p_{2,A} \end{aligned} \tag{22}$$

Here, the subscripts denote the chromosome type, so that $p_{12,X}$ is the proportion of divergent sites on the X that are heterozygous, and g_X and g_A are weightings, which should sum to one (Turelli and Orr 2000). Results for specific cases can then be derived from eq. 8.

In the following sections, we apply this approach to three patterns involving sex-specific hybrid breakdown, in species with heteromorphic sex chromosomes. The first pattern, in the F1, is well known (Haldane 1922; Turelli and Orr 2000). The other patterns were observed in backcross data, which were generated to uncover the genetic basis of F1 breakdown, and test reasonable hypotheses about its causes (Moehring 2011; Moran et al. 2017). Both of these patterns have been called surprising, because neither agreed with the hypotheses (Moehring 2011; Moran et al. 2017). We show that all three patterns are consistent with predictions from Fisher's geometric model.

2.3.2 Haldane's Rule

Haldane's Rule states that sex-specific F1 breakdown usually appears in the heterogametic sex (Haldane 1922; Turelli and Orr 2000). To show how Fisher's model predicts this pattern, we will assume an XO system for concreteness, such that females are homogametic, and males heterogametic. We will also assume that selection is identical in both sexes, and that pure-species males and females have the same fitness. These assumptions imply a form of dosage compensation, such that X-linked alleles have identical effects in homozygous or hemizygous state (Fraïsse et al. 2016b; Mank et al. 2011).

With these assumptions, the sole difference between male and female F1 is their heterozygosity. In XX females, all divergent sites are heterozygous, while in males, X-linked loci are hemizygous, such that $p_{12} = 1 - g_X$. From eq. 8 we therefore find

$$f_{\mathrm{F1}\female} = 0 \tag{23}$$

$$f_{\mathrm{F1}\male} = g_X - (1 - f_\mathrm{P})\, g_X^2 \tag{24}$$

So $f_{\mathrm{F1}\male} > f_{\mathrm{F1}\female}$ and Fisher's model yields Haldane's Rule (Barton 2001; Fraïsse et al. 2016b; Schiffman and Ralph 2017).

These results imply that female F1 will always have optimal fitness, regardless of the genetic distance between their parents (Barton 2001; Fraïsse et al. 2016b). However, if we extend the model, and allow for a proportion $g_\female$ ($g_\male$) of the divergence that is strictly maternally (paternally) inherited, then we find

$$f_{\mathrm{F1}\female} = g_\female + g_\male - (1 - f_\mathrm{P})\left(g_\female - g_\male\right)^2 \tag{25}$$

$$f_{\mathrm{F1}\male} = g_\female + g_\male - (1 - f_\mathrm{P})\left(g_\female - g_\male\right)^2 + g_X - (1 - f_\mathrm{P})\, g_X \left(g_X + 2g_\female - 2g_\male\right) \tag{26}$$

This still yields Haldane's Rule for realistic parameter values (it always holds when $g_\female < g_A$ for example), but breakdown can now appear in both sexes. This has two important consequences. First,

exceptions to Haldane's Rule can appear, but only in rare circumstances: when uniparentally-inherited loci act on traits that are subject to selection only in the homogametic sex (Fraïsse et al. 2016b). Second, from eqs. 2 and 5, as divergence increases, the fitness of all F1 hybrids will tend to decline; this yields an "F1 speciation clock" (Edmands 2002; Fraïsse et al. 2016b).

2.3.3 Male backcrosses of female F1

A surprising pattern in backcross data was observed by Moehring (2011). Moehring reanalyzed three data sets of reciprocal backcrosses from *Drosophila* species, namely *D. simulans/sechellia* (Macdonald and Goldstein 1999); *D. santomea/yakuba* (Moehring et al. 2006a,b); and *D. pseudoobscura/persimilis* (Noor et al. 2001). In all three cases, F1♂ had low fertility, consistent with Haldane's Rule, and so male hybrids were derived from the backcross F1♀ × P1♂. These backcross males vary in two measures of heterospecificity: their autosomal heterozygosity, $p_{12,A}$, and their heterospecificity on the X, $p_{2,X}$. Supplementary Figure S4 plots the data as a function of these two quantities.

Moehring (2011) predicted that sterility would correlate positively with $p_{2,X}$ and negatively with $p_{12,A}$. These predictions follow from reasonable assumptions about Haldane's Rule: that male sterility arises from partially recessive X-autosome interactions (Coyne and Orr 1989; Moehring 2011). Surprisingly, only one of these predictions was supported. Backcross sterility in all six crosses correlates positively with $p_{2,X}$, but correlations with $p_{12,A}$ are weak and inconsistent (see Supplementary Figure S4, and Table 3 of Moehring 2011).

Exactly this pattern is predicted by Fisher's geometric model. To see this, Figure 4a depicts the fitness surface for hybrid males, as a function of $p_{2,X}$ and $p_{12,A}$. Individuals from a given cross might occupy a rectangular region, whose bounds are determined by g_X. From annotated *Drosophila* genomes, we estimated that $g_X = 0.17$ might characterize the *simulans/sechellia* and *yakuba/santomea* pairs, and that $g_X = 0.37$ might characterize the *pseudoobscura/persimilis* pair (Table 1; see Methods for details). Figure 4 panels b-e show slices through the fitness surface for these values. In both cases, breakdown increases steadily with $p_{2,X}$, except in the improbable case that the recombinant autosomes were completely heterozygous (Fig. 3b-c). This is consistent with the positive correlations observed. By contrast, the dependencies on $p_{12,A}$ (Fig. 4d-e) vary in sign. This is consistent with the lack of consistent correlations with $p_{12,A}$ (Supplementary Figure S4).

Figure 4e also suggests a new testable prediction, which applies when g_X is large, as we have estimated for *D. persimilis/pseudoobscura* (Noor et al. 2001). When X-linked heterospecificity is low, then sterility is predicted to increase with $p_{12,A}$, but when X-linked heterospecificity is high, then sterility is predicted to decrease with $p_{12,A}$. With its two X-linked markers, the data of Noor et al. (2001) divide naturally into subsets with low, medium and high heterospecificity on the X (see the three rows of data points in Supplementary Figure S4e-f). Since we have no simple prediction when $p_{2,X}$ is intermediate, we excluded these individuals, and then fit a GLM to the remaining data. We treated $p_{12,A}$ as a linear predictor, and $p_{2,X} = 1$ versus $p_{2,X} = 0$ as a binary factor. In effect, we fit two linear regressions of sterility on $p_{12,A}$, with different intercepts and slopes for the high-$p_{2,X}$ and low-$p_{2,X}$ individuals. As shown in Table 3, the predictions of Fisher's model were supported for both backcross directions. Model selection favored a model with two slopes, and sterility correlated positively with $p_{12,A}$ when $p_{2,X} = 0$, and negatively with $p_{12,A}$ when $p_{2,X} = 1$.

2.3.4 Female backcrosses of male F1

A second surprising pattern in backcross data was observed by Moran et al. (2017). These authors studied the field crickets *Teleogryllus oceanicus* and *T. commodus*, which have XO sex determination, and a large X chromosome ($g_X \approx 0.3$; Moran et al. 2017). They are also a rare exception to Haldane's Rule, with F1 sterility appearing solely in XX females (Hogan and Fontana 1973). Moran et al. (2017) hypothesized that female sterility might be caused by negative interactions between heterospecific alleles on the X, which appear together in F1♀, but not in F1♂. To test this hypothesis, they compared two types of backcrosses, each with similar recombinant autosomes, and non-recombinant X chromosomes, in their pure species form. However, one backcross type carried two identical copies of the X, both from the same species; while the other type carried one copy of the X from each species (see Moran et al. 2017, or Appendix 4 for full details). If dominant X-X incompatibilities were present, these two backcross types should have differed markedly in fertility, but this was not observed: both backcrosses were less fertile than the F1, and there were no strong differences between them (see Figure 2 of Moran et al. 2017).

Again, this surprising result is consistent with predictions from Fisher's geometrical model. Full details are given in Appendix 4 and Supplementary Figure S5, but the key to the explanation lies in eq. 21. With well-adapted parents, heterozygosity in backcrosses is under symmetrical diversifying selection, and the two backcrosses of Moran et al. (2017) would have yielded heterozygosities with equal but opposite deviations from $p_{12} = \frac{1}{2}$. As such, they are predicted to show the same level of breakdown.

The explanation above is incomplete, because it neglects loci with uniparental inheritance, and without such loci, Fisher's model cannot explain the sterility observed in the F1♀ (compare eqs. 23 and 25 above). However, including uniparental inheritance does not qualitatively alter predictions for backcrosses. To see this, let us assume that a fraction $g_♀$ of the divergence is maternally inherited. In this case, we find

$$f_{\mathrm{F1}♀} = g_♀(1 - g_♀) \tag{27}$$

$$f_{\mathrm{BC}♀} = \frac{1 - g_X^2 - g_♀^2}{4} \pm \frac{g_X g_♀}{2} \tag{28}$$

where the sign of the correction term in eq. 28 depends on whether the X chromosomes come from the same species, or different species (see Appendix 4 for a full derivation). The implications of eqs. 27-28 are clearest from a numerical example. Let us assume that a fraction of the paternal X is silenced in females, such that $g_X = 0.2$ and $g_♀ = 0.1$; we would then have $f_{\mathrm{F1}♀} = 0.09$, and $f_{\mathrm{BC}♀} = 0.2375 \pm 0.01$. As such, eqs. 27-28 allow for substantial breakdown in the female F1, with stronger and similar breakdown in the two sets of backcrosses. This all agrees with the data from *Teleogryllus* (Moran et al. 2017).

2.4 Estimating the fitness surface

Across a diverse collection of hybrids, equation 9 predicts that the hybrid index will be under symmetrical disruptive selection, and heterozygosity under directional selection. This prediction can be tested with data sets containing estimates of fitness, h and p_{12} for many hybrid individuals. Exactly such an analysis was presented by Christe et al. (2016), for families of wild hybrids from the forest trees, *Populus alba* and *P. tremula* (Christe et al. 2016; Lindtke et al. 2012, 2014). These authors scored survival over four years in a common-garden environment, and fit a GLM to these binary data (binary logistic regression, with "family" as a random effect), and predictors including linear and quadratic terms in p_{12} and h. Model selection favored a four-term model, with terms in p_{12}, h, h^2 (see Supplementary Table S3, and Supplementary information of Christe et al. 2016 for full details). For comparison with our theoretical predictions, we can write their best fit model in the following form:

$$y = const + \beta_0 \left(\beta_1 h \left(1 - \beta_2 h\right) - p_{12}\right) \tag{29}$$

where y is the fitted value for hybrid breakdown. From eq. 9, Fisher's model predicts that $\beta_0 > 0$, $0 \geq \beta_1 \geq 4$, and $\beta_2 = 1$, should hold. The best-fit model of Christe et al. (2016) corresponds to $\hat{\beta}_0 = 2.963$, $\hat{\beta}_1 = 2.59$ and $\hat{\beta}_2 = 0.93$, which supports the predictions of directional selection toward higher heterozygosity, and near-symmetrical diversifying selection on the hybrid index.

To obtain confidence intervals on these parameters, we fit the model of eq. 29 to the raw data of Christe et al. (2016). We also searched for other data sets, from which we could estimate the hybrid fitness surface. After applying some quality controls (see Methods, and Supplementary Table S1), we identified one other data set of wild hybrids, from the mouse subspecies *Mus musculus musculus/domesticus*, where male testes size was the proxy for fertility (Turner and Harr 2014). We also found four data sets of controlled crosses: F2 from the same mouse subspecies (White et al. 2011), and the ragworts *Senecio aethnensis* and *S. chrysanthemifolius* (Chapman et al. 2016); and the *Drosophila* backcrosses discussed above (Macdonald and Goldstein 1999; Moehring et al. 2006a,b). Unlike the data from wild hybrids, these single-cross data sets leave large regions of the fitness surface unsampled; nevertheless, they each contain enough variation in h and p_{12} for a meaningful estimation. Details of all six data sets are shown in Table 1, and they are plotted in Supplementary Figures S6-S8.

Figure 5 shows a summary of the estimated parameters, and full results are reported in Supplementary Tables S2 and S3, and Supplementary Figures S6-S8. Taken together, the results show good support for the predictions of eq. 9. For all six data sets there was evidence of significant positive selection on heterozygosity ($\hat{\beta}_0 > 0$ was preferred in all cases). Furthermore, for all six data sets, we inferred diversifying selection acting on the hybrid index. Estimates of β_2, shown in the upper panel of Figure 5, show that this selection was near-symmetrical in all cases, such that $\hat{\beta}_2 \approx 1$. The poorest fit to the predictions was found for the *Drosophila* backcrosses, where estimates of β_1 were significantly greater than the predicted upper bound of $\beta_1 = 4$ (Fig. 5 lower panel). But these data sets were least suited to our purpose, because estimates of h and p_{12} depend strongly on our rough estimate of $g_X = 0.17$, and because they lack F2-like genotypes, from the center of the fitness surface (Figure 2a; Supplementary Figure S8). By contrast, results for the *Mus musculus* F2 (White et al. 2011), are remarkably close to the predictions of eq. 7 (Fig. 5; Supplementary Figure S7).

Two other features of the results deserve comment. First, for the two F2 data sets, it was not possible to provide meaningful confidence intervals for β_1 and β_2. This is because, for these two data sets, the terms in h and h^2 did not make a significant contribution to model fit, and so the preferred model contained only selection on p_{12} (see Supplementary Table S3). This is consistent with our earlier prediction of eq. 19, and stems from the low variation in $4h(1-h)$ among F2 hybrids (see Appendix 3 and Supplementary S6 and S7).

Second, for two of the data sets, *Populus* and *Senecio*, the estimates of β_1 are substantially lower than 4 (Figure 5; Supplementary Figure S6). This is suggestive of parental maladaptation, creating true heterosis in the hybrids (see eq. 9). Consistent with this inference, there is independent evidence of F1 hybrid vigor in both species pairs (*Populus*: Caseys et al. 2015; *Senecio*: Abbott and Brennan 2014).

3 Discussion

In this article, we have used Fisher's geometric model to develop predictions for the relative fitness of any class of hybrid. The modeling approach is simple, with few free parameters, and it generates a wide range of testable predictions. We have tested some of these predictions with new and published data sets (Table 1), and the major predictions of the model are well supported.

We emphasize that our approach is designed for coarse-grained patterns in the data, and typical outcomes of the evolutionary process, without considering the particular set of substitutions that differentiate the parental lines. The limitations of such an approach are seen in the low r^2 values associated with our model fitting (Supplementary Table S2); and in empirical patterns that eq. 9 could not hope to explain. For example, there are often strong fitness differences between the reciprocal F1 (Turelli and Moyle 2007), and Fisher's model can generate such asymmetries with uniparental inheritance (Fraïsse et al. 2016b), but if P1 and P2 are equally fit, then the expected breakdown must be the same for both cross directions, and only the expected breakdown has been considered in the present work. These limitations notwithstanding, our approach should enable novel and complementary uses of genomic data sets, which do not depend on identifying individual loci with anomalous effects. Such a genome-wide interpretation of hybrid fitness is essentially lacking in the "speciation genes" framework.

A second goal of the present work was to show how Fisher's model can interpolate between previous modeling approaches, namely the classical theory of inbreeding (Crow 1952; Wright 1922), and models of genetic incompatibilities, involving a small number of loci (Dobzhansky 1937; Gavrilets 2004; Orr 1995; Welch 2004). We have also shown that Fisher's model can account for empirical patterns that each approach has struggled to explain, although there are caveats to note in each case.

With inbred lines of *Zea mays*, we showed how observed differences in hybrid vigor between the BC and F2 are expected, if we allow for a limited degree of coadaptation between the alleles that differentiate the lines (Figure 3; Wright 1977). The major caveat in this case is our simplifying assumption that the midparent is optimal (eq. 9; Appendix 1). This assumption is consistent with the *Zea* data, which show an enormous increase in F1 yield, but it is not clear how often the assumption would be met under an explicit model of mutation accumulation.

With the backcross data from *Drosophila* and *Teleogryllus*, the situation is more complicated. Moehring (2011) and Moran et al. (2017) showed that their data were not consistent with predictions from simple

models of incompatibilities. But while these models were based on very reasonable assumptions, they only included incompatibilities of a single type (partially recessive X-A incompatibilities to explain Haldane's Rule in *Drosophila*, or dominant X-X incompatibilities to explain the exception to Haldane's Rule in *Teleogryllus*). We have shown that Fisher's geometric model gives identical predictions to a general model of incompatibilities (eqs. 11-14), and that this general model can account for the patterns observed. It is also clear that the predictions were much more easily generated with eq. 6 than with eq. 13. In this case, there are two major caveats. First, the two models give identical predictions only when the dominance relations of incompatibilities are assigned in a particular way (eq. 14). But we have argued that these parameter values are biologically realistic, and strongly implied by other well-established empirical patterns (Appendix 2; Turelli and Orr 2000). Second, even when predictions are identical for the quantity f (eq. 2), the two approaches still make different predictions for other kinds of data, and these were not considered in the present work. The most important difference is the dependency of log fitness on d, the genomic divergence between the species. Under Fisher's geometric model, the log fitness of hybrids declines with $-d^{\beta/2}$ (eqs. 1-2 and 5). By contrast, with the simplest models of incompatibilities, there is a snowball effect (Orr 1995), where the number of incompatibilities grows with d^{ℓ} (eq. 11), and so log fitness declines with $-d^{\ell\beta/2}$. This is a genuine difference between the modeling approaches, although truly discriminatory tests may be difficult (Fraïsse et al. 2016b). For example, it may not always be possible to distinguish between an incompatibility-based model with a low value of β (equivalent to strong positive epistasis between incompatibilities), or a model where β is higher, but where the number of "incompatibilities" does not snowball, because they appear and disappear as the genetic background changes (Fraïsse et al. 2016b; Guerrero et al. 2017; Kalirad and Azevedo 2017; Welch 2004).

Given the simplicity and flexibility of the modeling approach explored here, and its predictive successes with a range of data, it should be readily extendable to address other outstanding questions in the study of hybridization. These include the putative role of hybridization in adaptive evolution (e.g. Duranton et al. 2017; Fraïsse et al. 2016a,b; Mendez et al. 2012), the effects of recombination in shaping patterns of divergence (Schumer et al. 2017), and the roles of intrinsic versus extrinsic isolation (Chevin et al. 2014). Given its ability to interpolate between models of different and extreme kinds, it should also be particularly useful for understanding hybridization in intermediate regimes, where parental genomes are characterized by both maladaptation and allelic coadaptation, or where the architecture of isolation involves many genes of small or moderate effect (Baird 2017; Boyle et al. 2017; Buerkle 2017; Davis and Wu 1996; Maside and Naveira 1996; Morán and Fontdevila 2014).

4 Methods

4.1 *Mytilus* data

Conserved tissues from the mussel species, *Mytilus edulis* and *Mytilus galloprovincialis,* and their hybrids, were retained from the work of Bierne et al. (2006, 2002). As reported in those studies, *M. edulis* from the North of France were crossed with *M. galloprovincialis* from the French Mediterranean coast to produce F1 hybrids (five males and one female; Bierne et al. 2002). The F1 were then used to produce an F2, and sex-reciprocal backcrosses to *M. galloprovincialis* (which we denote here as BC_{12} and BC_{21}; Bierne

et al. 2006). In particular, oocytes from the F1 female were fertilized by the pooled sperm of the five F1 males producing F2 individuals, from which 132 individuals were sampled; oocytes from the F1 female were fertilized by pooled sperm of five *M. galloprovincialis* males to produce BC_{12}, from which 72 individuals were sampled; and five *M. galloprovincialis* females were fertilized by pooled sperm from the five F1 males, producing BC_{21}, from which 72 individuals were sampled. In addition to these hybrids, we also genotyped 129 individuals from "reference" populations of the two species, found in regions with relatively little contemporary introgression. In particular, we sampled *M. galloprovincialis* from Thau in the Mediterranean Sea; and sampled *M. edulis* from four locations in the North Sea and English Channel (The Netherlands, Saint-Jouin, Villerville and Réville). Full details of these reference populations are found in Supplementary Table S4.

In each case, gill tissues were conserved in ethanol at -20° C. DNA was extracted using a NucleaMag 96 Tissue kit (Macherey-Nagel) and a KingFisher™ Flex (ThermoFisher Scientific). We then genotyped all samples for 98 *Mytilus* markers that were designed from the data of Fraïsse et al. (2016a). The flanking sequences of the 98 SNPs are provided in Supplementary Table S5. Genotyping was sub-contracted to LGC-genomics and performed with the KASP™ chemistry (Kompetitive Allele Specific PCR, Semagn et al. 2014). Results are shown in Supplementary Figure S3. Many of the 98 markers are not diagnostic for *M. edulis* and *M. galloprovincialis*, and so we retained only the 43 that were scored as heterozygous in all 6 of the F1 hybrids. To obtain a reduced set of strongly diagnostic markers, we measured sample allele frequencies in our pure species *M. edulis* and *M. galloprovincialis* samples (pooling *M. edulis* individuals across the four sampling locations; Supplementary Table S4), and retained only markers for which the absolute difference in allele frequencies between species was >90%. This yielded the set of 33 markers used for the right-hand columns in Table 2. The "subsampled" data shown in the fourth column of Table 2, excluded any BC hybrid who carried the major allele typical of *M. edulis* in homozygous form. This yielded 56 BC hybrids. We then retained the first 56 F2 to be sequenced, to equalize the sample sizes.

4.2 Collation of published data

We searched the literature for published data sets combining measures of individual hybrid fitness, with genomic data that could be used to estimate p_1, p_2 and p_{12}. In addition to those shown in Table 1, we also examined data sets that proved unsuitable for the sort of reanalysis presented here. These included data sets where the measure of fecundity or fertility took an extreme low value for one of the pure species, suggesting that it is not a good proxy for fitness (e.g. Orgogozo et al. 2006), data where the fitness proxy correlated strongly with a measure of genetic abnormality such as aneuploidy (Xu and He 2011), or data where the states of many markers could not be unambiguously assigned, for example, due to shared variation. Before estimating the fitness surface, we also excluded any data set where there was a highly significant rank correlation between the proportion of missing data in an individual, and either their heterozygosity, or fitness. For this reason, we did not proceed with reanalyses of the excellent data sets of Li et al. (2011), or Routtu et al. (2014) (see Supplementary Table S1 for full details). For our reanalysis of the *Mus musculus* F2 (White et al. 2011), we used a conservative subset of these data; we excluded any individual where any X-linked marker was scored as heterozygous (indicative of sequencing errors in heterogametic males; White et al. 2011), and controlled for variation in the

uniparentally inherited markers, by retaining only individuals carrying *M. m. domesticus* mitochrondria, and the *M. m. musculus* Y. However, results were little changed when we used all 304 individuals with sterility data (Supplementary Table S3). Results were also unaffected when we used alternative proxies for fitness (Supplementary Table S3).

4.3 Estimation of g_X from annotated genomes

For taxa with XY sex determination (Table 1), the weightings g_X and g_A, which determine the contribution of the X and autosomes to the overall constitution of the genome (eqs. 22), were estimated from the total length of coding sequences associated with each chromosome type, ignoring the small contributions from the Y and mitochondria. In each case, we obtained the longest protein product for each unique gene, and then summed their lengths, using a custom R script. The g_X values, shown in Table 1, were calculated as the total length of X-linked CDS divided by the total CDS length. For *Mus musculus*, we used the reference genome assembly "GRCm38.p5". For *Drosophila simulans*, we used the assembly "GCA_000754195.3 ASM75419v2", and for *Drosophila yakuba* "GCA_000005975.1 dyak_caf1". For *Drosophila pseudoobscura*, the current annotation was downloaded from FlyBase release 3.04 (Gramates et al. 2017). The .gtf file was then sorted and merged (combining overlapping coding sequences on each chromosome) using BEDTools (Quinlan and Hall 2010). Coding sequence lengths were calculated and summed over each chromosome, using custom awk commands.

4.4 GLM methods

The linear model results shown in Table 3, Figure 5, Supplementary Tables S2 and S3, and Supplementary Figures S6-S8, were all fit in R v. 3.3.2 (R Core Team 2016). For data sets with quantitative fitness measures (Turner and Harr 2014; White et al. 2011; Supplementary Figure S7) we used the standard general linear models, with Gaussian errors, and chose data transformations to reduce heteroscedasticity. For binary fitness data (Chapman et al. 2016; Christe et al. 2016; Noor et al. 2001; Table 3; Supplementary Figure S6), we used binomial regression with a logit link implemented in the *glm* function; and with ordinal fitness data (Macdonald and Goldstein 1999; Moehring et al. 2006b; Supplementary Figure S8) we used proportional odds logistic regression (Agresti 2003), implemented in the *polr* function. In these cases, the *p*-values shown in Supplementary Table S3 were calculated by comparing the *t*-value to the upper tail of normal distribution, as in a Wald test. For the non-Gaussian models, we also report McFadden's pseudo-r^2, defined as one minus the ratio of log likelihoods for the fitted and null models (McFadden 1974).

Acknowledgments

We are very grateful indeed to all of the authors of the original data reanalyzed here. We are especially grateful to the following for providing clarifications or reformatted data: Luisa Bresadola, Prof. E. Charles Brummer, Dr. Mark A. Chapman, Dr. Camille Christe, Prof. Eric Hagg, Prof. Xionglei He, Prof. Christian Lexer, Prof. Xuehui Li, Prof. Amanda Moehring, Prof. Bret Payseur, Prof. Michael

White, and Dr. Gavin Woodruff. We are also grateful to Andrea Betancourt for advice on processing the genome annotations.

Appendix 1: the random walk approximation with suboptimal parental types

In this Appendix, we derive the random walk approximation for the breakdown score of a given hybrid genotype, under Fisher's geometric model. Let us begin by describing the two parental phenotypes as n-dimensional vectors, denoted $\mathbf{z}_{\mathrm{P1}}$ and $\mathbf{z}_{\mathrm{P2}}$, which are equal but opposite deviations from the mid-parental phenotype, denoted as $\mathbf{z}_{\mathrm{mp}}$. So if we define

$$\mathbf{z}_{\mathrm{mp}} \equiv \frac{\mathbf{z}_{\mathrm{P1}} + \mathbf{z}_{\mathrm{P2}}}{2} \tag{30}$$

$$\mathbf{r} \equiv \frac{\mathbf{z}_{\mathrm{P1}} - \mathbf{z}_{\mathrm{P2}}}{2} \tag{31}$$

then

$$\mathbf{z}_{\mathrm{P1}} = \mathbf{z}_{mp} + \mathbf{r} \tag{32}$$

$$\mathbf{z}_{\mathrm{P2}} = \mathbf{z}_{mp} - \mathbf{r} \tag{33}$$

Below, we will use the notation $z_{\mathrm{mp},i}$ and r_i to refer to the components of these vectors for trait i.

We can now consider the d mutations that differentiate P1 and P2 as describing equal but opposite paths from one of the parental phenotypes, to the midparent. Our approximation is to treat this path, on each of the n traits, as a Brownian bridge.

To derive this approximation, let $B(t)$ denote a Brownian bridge, taking place over a single unit of time, such that $0 \leq t \leq 1$, and with a rate σ_B. $B(t)$ is normally distributed, with the following mean:

$$E\left(B(t)\right) = B(0) + t\left(B(1) - B(0)\right) \tag{34}$$

and covariance at two time points given by:

$$\mathrm{Cov}\left(B(t_1), B(t_2)\right) = \sigma_B^2\left(1 - t_2\right)t_1, \qquad 0 \leq t_1 \leq t_2 \leq 1 \tag{35}$$

To model hybrid genotypes, we will need to count some sections of the random walk twice, to account for any homozygous alleles, and some sections only once, to account for any heterozygous alleles. Therefore, we are interested in the quantity:

$$B_{hyb} \equiv B\left(t_1 + t_2\right) + B\left(t_1\right) \tag{36}$$

From eqs. 34-35, B_{hyb} will also be normal, with the following mean and variance

$$E\left(B_{hyb}\right) = 2B(0) + \left(2t_1 + t_2\right)\left(B(1) - B(0)\right) \tag{37}$$

$$\text{Var}\left(B_{hyb}\right) = \sigma_B^2\left\{t_1(1-t_1) + (t_1+t_2)(1-t_1-t_2) + 2(1-t_1-t_2)t_1\right\}$$

We can now apply these results to z_i, the deviation from the optimum of trait i (see eq. 4 in the main text). In this case, the random walk begins from the trait value of parent P1: $B(0) = z_{\text{mp},i} + r_i$, ends at the midparent: $B(1) = z_{\text{mp},i}$, and has a total rate equal to the total number of mutations, multiplied by their typical effect size: $\sigma_B^2 = d\, v_i$. We then take the intermediate timepoints to be $t_1 = p_2$ (this section of the walk is counted twice, to account for homozygous alleles), and $t_2 = p_{12}$ (this section is counted once, to account for heterozygous alleles).

Putting these results together, we find that z_i is a normally distributed random variable, with the following properties:

$$z_i \sim N(\mu_i, \sigma_i^2) \tag{38}$$

$$\tag{39}$$

$$\sigma_i^2 = d\, v_i\ \left(p_{12}(1-p_{12}) + 4p_1p_2\right) \tag{40}$$

$$\mu_i = z_{\text{mp},i} + \left(p_1 - p_2\right) r_i \tag{41}$$

From eq. 4, the breakdown score, S, depends on the squared trait values, and from normal theory, we have

$$E\left(z_i^2\right) = \sigma_i^2 + \mu_i^2 \tag{42}$$

$$\text{Var}\left(z_i^2\right) = 2\sigma_i^2\left(\sigma_i^2 + 2\mu_i^2\right) \tag{43}$$

As such, S will be approximately gamma distributed, with a mean and variance given by the weighted sum of these quantities.

Let us now consider the special cases discussed in the main text. First, and simplest, is the case where both parents, and therefore the midparent, are phenotypically optimal. This implies that all $z_{\text{mp},i} = 0$ and all $r_i = 0$, such that all $\mu_i = 0$. We then find

$$f \equiv \frac{E\left(S\right)}{E\left(S_+\right)} = \frac{\sum_i\ \lambda_i\, \sigma_i^2}{\sum_j \lambda_j\, d\, v_j} \tag{44}$$

And this yields eqs. 6-7 of the main text. Next, let us consider the case where the midparent is optimal (all $z_{\mathrm{mp},i} = 0$), but both parents are equally maladapted (some $r_i > 0$). In this case, $\mu_i^2 = (p_1 - p_2)^2 r_i^2$ and $S_{\mathrm{P}} = \sum \lambda_i r_i^2$, and so we find:

$$\begin{aligned} f &= p_{12}(1 - p_{12}) + 4p_1p_2 + (p_1 - p_2)^2 f_{\mathrm{P}} \\ &= 4h(1-h) - p_{12} + (1-2h)^2 f_{\mathrm{P}} \end{aligned} \tag{45}$$

which yields eqs. 8-9 of the main text.

Let us finally consider another simple case, in which one of the parental species (P2) is maladapted, while the other (P1) is optimal. In this case, we can set $z_{\mathrm{P1},i} = 0$ and $z_{\mathrm{P2},i} = r_i$, such that $z_{mp,i} = r_i/2$. We now have $\mu_i = (1 + p_2 - p_1)\,\frac{r_i}{2}$, and so

$$\begin{aligned} \frac{E(S)}{E(S_+)} &= p_{12}(1 - p_{12}) + 4p_1p_2 + (1 + p_2 - p_1)^2 \frac{f_{\mathrm{P1}}}{4} \\ &= 4h(1-h) - p_{12} + h^2 f_{\mathrm{P1}} \\ &= 4h\left(1 - \left(1 - \frac{f_{\mathrm{P1}}}{4}\right)h\right) - p_{12} \end{aligned} \tag{46}$$

Comparing eq. 46 to eq. 7 shows that maladaptation in one of the parental species introduces an asymmetry in the selection on the hybrid index, h, but leaves the form and strength of selection on heterozygosity p_{12} unchanged. This situation is illustrated in Supplementary Figure S1d.

Appendix 2: The dominance relations of incompatibilities

In this Appendix, we consider incompatibility-based models of hybrid fitness (eqs. 11-13). We examine different ways of assigning the parameters, s_{ijk}, which appear in f_I (eq. 13), and represent the expected contribution to hybrid breakdown of individual incompatibilities, and especially, their dominance or recessivity (Turelli and Orr 2000). To understand this, let us begin by assigning the following functional form:

$$s_{ijk} \propto \left(\frac{1}{2}\right)^{\delta k} \tag{47}$$

where below, we will use the constant of proportionality $2\left(2^{\ell} - 2\right)$, to simplify the algebra. In eq. 47, the parameter δ allows us to tune the dominance of incompatibilities, measured in terms of breakdown score, rather than fitness. When $\delta = 1$, then each heterozygous locus halves the effects of incompatibility. This is equivalent to assuming that incompatibilities act multiplicatively, since each heterozygous locus halves the number of times that the incompatible combination of alleles is present in the genome. The s_{ijk} under multiplicative selection ($\delta = 1$) are illustrated by the green points in Supplementary

Figure S2.

To determine the predictions of this model, let us substitute eq. 47 into eq. 13, and set $\delta = 1$. After some algebra, we find:

$$f_I = 2\left[1 - \left(p_2 + \tfrac{1}{2}p_{12}\right)^\ell - \left(p_1 + \tfrac{1}{2}p_{12}\right)^\ell\right], \qquad \delta = 1 \tag{48}$$

$$\equiv 2\left[1 - h^\ell - (1-h)^\ell\right] \tag{49}$$

where h is the hybrid index, as defined in eq. 3. As such, when incompatibilities act multiplicatively, breakdown will depend solely on the total heterospecificity, and not at all on how the heterospecific alleles are arranged into genotypes (i.e. whether they appear as homozygotes or heterozygotes). It follows that breakdown is not predicted to change between the F1 and F2 crosses, and that homogametic F1, with $h = \frac{1}{2}$, will have the highest possible breakdown score. As such, this multiplicative model cannot predict hybrid breakdown between the F1 and F2, or Haldane's Rule.

Now let us consider another extreme assumption. We assume that incompatibilities are fully recessive, such that no breakdown appears unless all incompatible alleles appear in homozygous or hemizygous form. We model this by making δ very large, such that $s_{ijk} = 0$ unless $k = 0$. These values are illustrated by the red points in Supplementary Figure S2. With the assumption of complete recessivity, we find:

$$f_I = 2\left[(p_1 + p_2)^\ell - p_1^\ell - p_2^\ell\right], \qquad \delta \to \infty \tag{50}$$

Equation 50 does not predict Haldane's Rule, unless there is substantial uniparental inheritance from both the male and female parents. This is because $f_I = 0$ if $p_1 p_2 = 0$, and so both male and female F1 will have identical and optimal fitness. For similar reasons, eq. 50 predicts that the fitness of heterogametic backcrosses will decrease with $p_{12,A}$: a prediction that is not supported by the relevant data (Moehring 2011).

We have shown that both extreme regimes (no recessivity, and complete recessivity) yield unsupported predictions. But what values of δ are biologically plausible? To answer this question, let us consider Haldane's Rule under an incompatibility-based model, and ignoring uniparental inheritance. Assuming that males are heterogametic, Haldane's Rule will hold when

$$f_{I,\mathrm{F1}\male} > f_{I,\mathrm{F1}\female} \tag{51}$$

and using eqs. 13 and 47, after some algebra, eq. 51 is found to be equivalent to:

$$(1 - g_X)^\ell + \left(1 - g_X + 2^\delta g_X\right)^\ell - \left(2(1 - g_X) + 2^\delta g_X\right)^\ell > 2^\ell - 2 \tag{52}$$

This condition is most difficult to satisfy when incompatibilities involve two loci ($\ell = 2$), and in this

case, we find the solution:

$$\delta > \ln\left(\frac{2-g_X}{1-g_X}\right)/\ln(2) \tag{53}$$

The value of δ that is required to yield Haldane's Rule will therefore increase with g_X. Towards the limit of the biologically plausible range, when two-thirds of the between-species divergence is X-linked ($g_X = 2/3$) Haldane's Rule will hold only if $\delta > 2$. As such, setting $\delta = 2$, such that each heterozygous locus reduces the breakdown score by a factor of four, will yield Haldane's Rule in most cases. The s_{ijk} values from eq. 47 with $\delta = 2$ are shown as yellow points in Supplementary Figure S2. Another feature of the model with $\delta = 2$ is that it produces parameter dependencies that are very close to those predicted by Fisher's geometrical model (see also Manna et al. 2011). The similarity is clearest with two-locus incompatibilities, where we find

$$\begin{aligned} f_I &= \left(\tfrac{1}{2}\right)^{\delta-2} p_{12}\left(1 - p_{12}\left[1 - \left(\tfrac{1}{2}\right)^{\delta}\right]\right) + 4p_1p_2, \qquad \ell = 2 \\ &= p_{12}\left(1 - \tfrac{3}{4}p_{12}\right) + 4p_1p_2, \qquad \ell = 2,\ \delta = 2 \end{aligned} \tag{54}$$

Comparing eq. 54 to eq. 6, shows that $f_I \approx f$ when we use eq. 47 with $\delta = 2$.

This is made even clearer when we compare the yellow points in Supplementary Figure S2, to the s_{ijk} values derived from eq. 14 of the main text, which were chosen to exactly match the predictions as Fisher's geometric model (i.e. the values which yield $f_I = f$). These s_{ijk} are shown as blue points in Supplementary Figure S2. The plot therefore clarifies the biologically-realistic assumptions embodied in eq. 14. First, these values reproduce the intermediate levels of recessivity that are required to generate Haldane's Rule. Second, eq. 14 states that incompatibilities will have stronger effects when alleles from both parental species appear in homozygous state. For example, if the three alleles ABc form an incompatibility (with upper and lower case letters distinguishing alleles from P1 and P2), then eq. 14 predicts that the genotype Aa/BB/cc (with $ijk = 111$) will tend to have lower fitness than the genotype AA/BB/Cc (with $ijk = 201$) even though both genotypes contain the incompatibility, and both comprise two homozygous loci and one heterozygous locus.

Appendix 3: Segregation and recombination

For a recombinant cross, such as the F2, the heterozygosity and hybrid index will vary between individuals. As such, to derive the expected breakdown score for a recombinant cross, we need to treat f (eq. 2) as a random variable. Because h and p_{12} may correlate strongly, it is convenient to define q as the "homozygous hybrid index": the proportion of homozygous divergent sites that originate with P2.

$$q \equiv \frac{p_2}{p_1 + p_2} = \frac{p_2}{1 - p_{12}} \tag{55}$$

If we assume that P1 and P2 are optimally fit, then using eqs. 6 and 55, we can write f as

$$f = p_{12}\left(1 - p_{12}\right) + 4q\left(1 - p_{12}\right)\left(1 - p_{12} - q\left(1 - p_{12}\right)\right) \tag{56}$$

such that

$$E\left(f\right) = \left(1 - \bar{p}_{12}\right)\left(\bar{p}_{12}\left(1 - 2\bar{q}\right)^2 + 4(1 - \bar{q})\bar{q}\right) - V_p\left(1 - 2\bar{q}\right)^2 - 4V_q\left(\left(1 - \bar{p}_{12}\right)^2 + V_p\right) \tag{57}$$

where

$$\begin{aligned}\bar{p}_{12} &\equiv E\left(p_{12}\right)\\ \bar{q} &\equiv E\left(q\right)\\ V_p &\equiv \mathrm{Var}\left(p_{12}\right)\\ V_q &\equiv \mathrm{Var}\left(q\right)\end{aligned}$$

and we have used the fact that q and p_{12} will not generally covary. This expression simplifies for special cases. For example, consider the standard crosses, with strictly biparental inheritance. For backcrosses, all homozygous sites must come from a single species, such that $\bar{q} = V_q = 0$, and for the first backcross, we have $\bar{p}_{12} = \frac{1}{2}$, and so

$$\begin{aligned}E\left(f_{\mathrm{BC}}\right) &= \bar{p}_{12}(1 - \bar{p}_{12}) - V_p\\ &= \frac{1}{4} - V_p\end{aligned} \tag{58}$$

For the F2, we have $\bar{p}_{12} = \bar{q} = \frac{1}{2}$, and so

$$E\left(f_{\mathrm{F2}}\right) = \frac{1}{2} - V_q - 4V_qV_p \tag{59}$$

V_p and V_q will depend on the distribution of the divergence across the genome, and on patterns of segregation and recombination. However, we can derive simple and useful predictions if we assume that the divergence is equally distributed among m freely recombining regions. These variances will also apply to estimators of p_{12} and q from m independently segregating markers. In this case, p_{12}, p_1 and p_2 follow a multinomial distribution, such that

$$V_p = \frac{\bar{p}_{12}(1 - \bar{p}_{12})}{m} \tag{60}$$

$$V_q \approx \frac{\bar{q}(1 - \bar{q})}{m(1 - \bar{p}_{12})}, \qquad m \gg 1 \tag{61}$$

where the last expression is approximate, because V_q is undefined if any individual is completely heterozygous, with $p_{12} = 1$. From these expressions, it follows that

$$E\left(f_{\mathrm{BC1}}\right) = \frac{1}{4}\left(1 - \frac{1}{m}\right) \tag{62}$$

$$E\left(f_{\mathrm{F2}}\right) \approx 2E\left(f_{\mathrm{BC1}}\right) + O(m^{-2}) \tag{63}$$

and so the predicted breakdown in the F2 is roughly double that of the first backcross. Similar considerations were used to derive the approximation of eq. 19, since in the F2, $\mathrm{Var}\left(4h(1-h)\right) \approx 1/(2m^2)$, and so most of the variance in f will come from $\mathrm{Var}\left(p_{12}\right) \equiv V_p = 1/(4m)$.

Appendix 4: Predictions for the *Teleogryllus* backcrosses

In this Appendix we provide a full derivation of the results for homogametic female backcrosses, which are relevant to the study of Moran et al. (2017) on *Teleogryllus* field crickets. Given the female-specific F1 sterility observed in *Teleogryllus*, Moran et al. (2017) generated backcrosses from males of the reciprocal F1. These hybrids are denoted $\mathrm{F1}_{12}$♂ (P1♀ × P2♂) and $\mathrm{F1}_{21}$♂ (P2♀ × P1♂). They differ solely in their X chromosomes, with $\mathrm{F1}_{12}$♂ carrying the X from P1, and $\mathrm{F1}_{21}$♂ carrying the X from P2. When these F1 are crossed with the parental lines, the female offspring form the reciprocal backcrosses: BC_{12}♀ ($\mathrm{F1}_{12}$♂ × P1♀) and BC_{21}♀ ($\mathrm{F1}_{21}$♂ × P1♀). These two backcross directions will both carry recombinant autosomes, for which $E\left(p_{12,A}\right) = \frac{1}{2}$ and $p_{2,A} = 0$. However, BC_{12}♀ will carry two identical copies of the X, while BC_{21}♀ will carry one X from each species. As such they are maximally different in their X-linked heterozygosity: $p_{12,X} = 0$ for BC_{12}♀ and $p_{12,X} = 1$ for BC_{21}♀. If we begin by ignoring uniparental inheritance, then the heterozygosities for the two backcross directions are $p_{12} = g_A p_{12,A}$ and $p_{12} = g_A p_{12,A} + 1 - g_A$. If we further assume that the parental types are well adapted, compared to the worst possible class of hybrid, then heterozygosity in both backcrosses will be under symmetrical diversifying selection, $f = p_{12}(1 - p_{12})$ (eq. 21). The two breakdown scores are therefore:

$$\begin{aligned} f_{\mathrm{BC}_{12}\text{♀}} &= g_A p_{12,A}\left(1 - g_A p_{12,A}\right) \\ f_{\mathrm{BC}_{21}\text{♀}} &= g_A\left\{1 - p_{12,A}\right\}\left(1 - g_A\left\{1 - p_{12,A}\right\}\right) \end{aligned} \tag{64}$$

These two values will be equal at the Mendelian expectation of $p_{12,A} = \frac{1}{2}$, and deviations from these expectations, due to stochasticity in segregation and recombination, will have equal but opposite effects for the two backcross directions, leading to identical predicted fitnesses overall. This is illustrated in Supplementary Figure S5, which shows the predicted fitness surfaces for homogametic backcrosses. The dashed lines in both panels represent the "mirror-image" fitness curves that apply to BC_{12}♀ and BC_{21}♀.

If we now assume that a fraction, $g_{\text{♀}}$, of divergent sites are subject to exclusively maternal inheritance, then the heterozygosity for BC_{12}♀ remains as $p_{12} = g_A p_{12,A}$, while for BC_{21}♀ it becomes $p_{12} = g_A p_{12,A} + 1 - g_A - g_{\text{♀}}$. These values yield eq. 28 of the main text, and the new fitness curve

for $BC_{21}♀$ is illustrated by the solid line in the lower panel of Supplementary Figure S5. We also note that the rough similarity in the breakdown scores for the two backcross directions applies only to the first backcross, and not to later backcrosses, for which $E\left(p_{12,A}\right) < \frac{1}{2}$. It is therefore notable that Moran et al. (2017) did find significant differences between backcross directions for their BC2 data (see their Table 3), again, consistent with predictions from Fisher's geometric model.

Tables and Figures

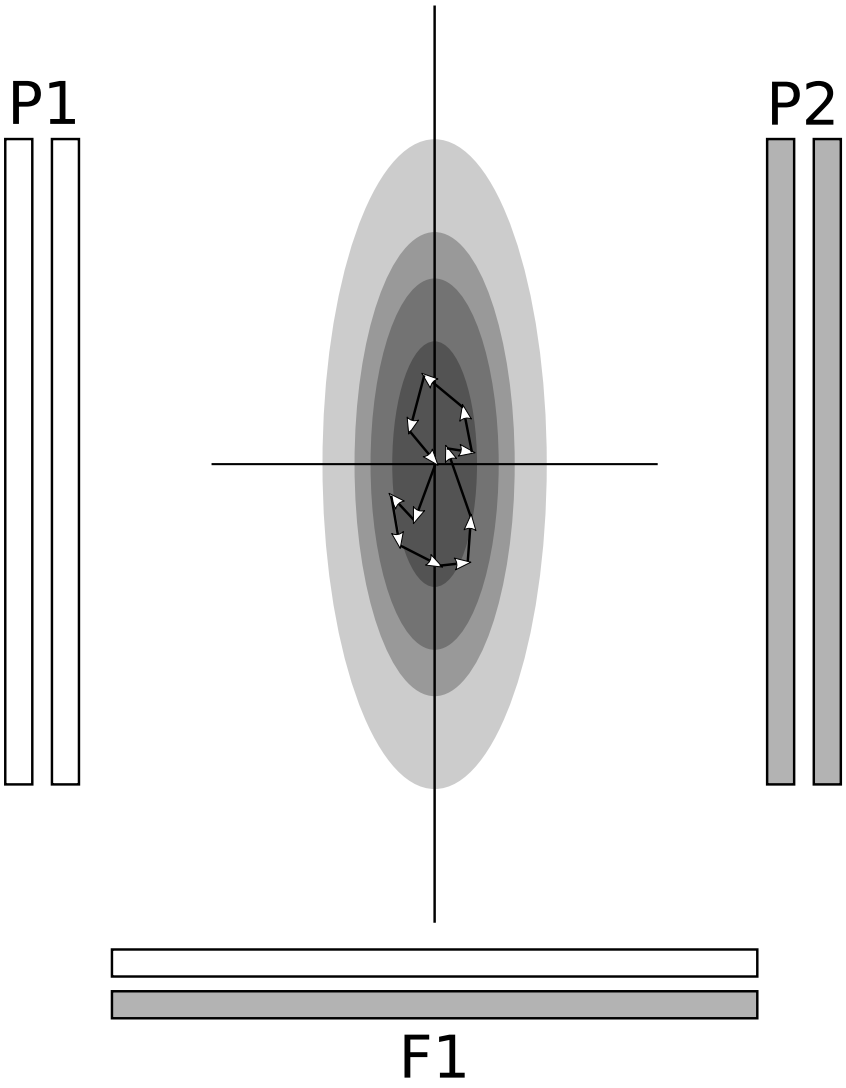

Figure 1: A schematic representation of Fisher's geometric model, with $n = 2$ "traits", each under optimizing selection of differing strengths. We consider hybrids between two diploid parental lines, P1 and P2, both of which have an optimal phenotype, but realized by different alleles. If we assume strict biparental inheritance, and additivity at the level of phenotype, then the initial F1 hybrid will have the midparental phenotype, which is also optimal. The expected fitness of other hybrids can be predicted by assuming that their component alleles form tethered random walks (Brownian bridges), between the three well-fit genotypes (see Appendix 1 for details).

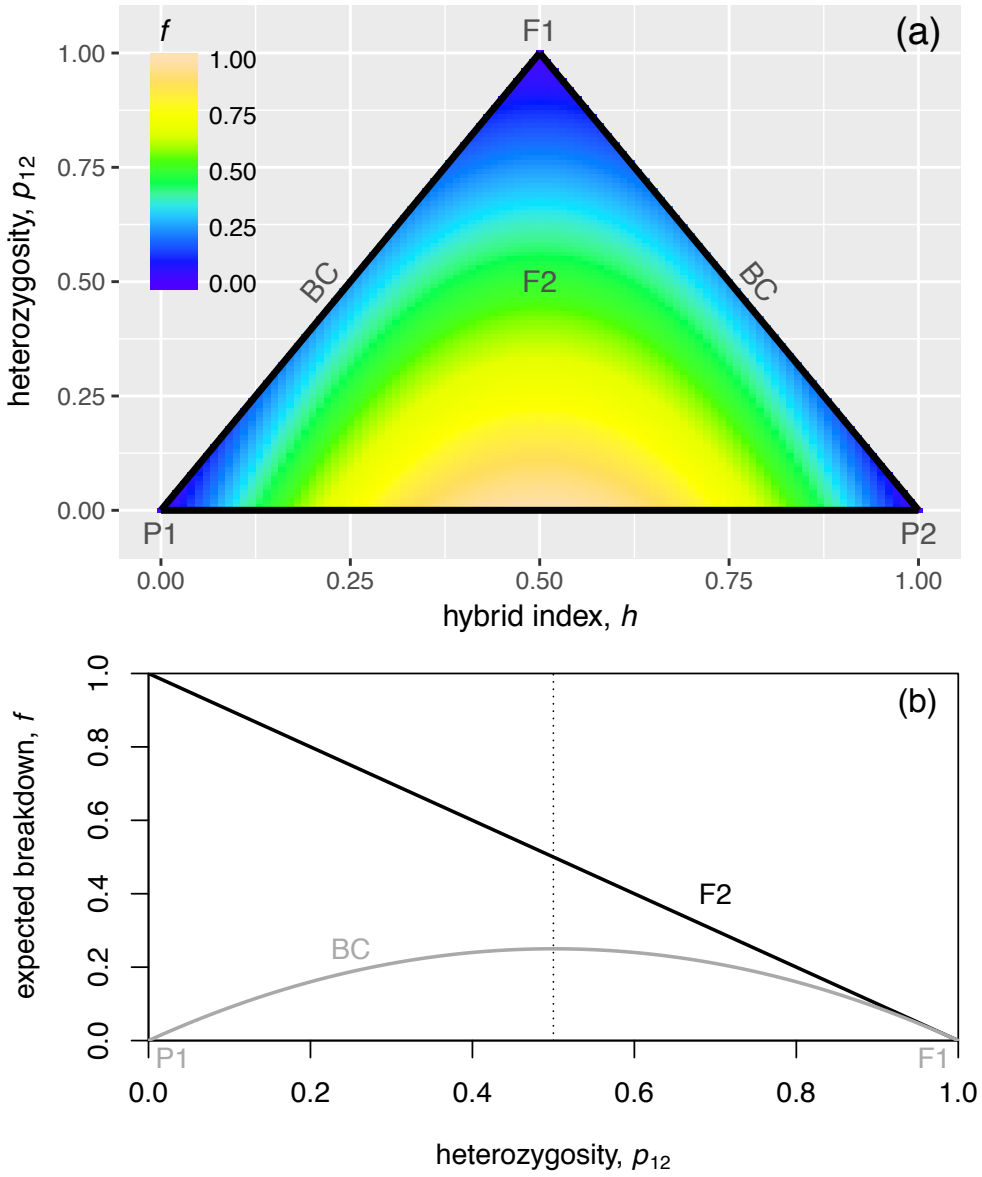

Figure 2: Panel (a) shows a heatplot of the fitness surface predicted by Fisher's geometric model, for hybrid genotypes, when the parental types are well adapted (eq. 7 with $f_{\mathrm{P}} = 0$). The colors represent the relative expected breakdown score, f, with higher values corresponding to lower fitness (eqs. 1-2). Predictions are shown as a function of the interspecies heterozygosity, p_{12} and the hybrid index, h (eq. 3). The parental P1 and P2, are found at the lower corners, with $p_{12} = 0$ and $h = 0$ or $h = 1$. With purely biparental inheritance, an initial F1 cross would be at the upper corner, with $p_{12} = 1$, backcrosses would lie along the upright edges, with $h = p_{12}/2$ or $h = 1 - p_{12}/2$, and the F2 would cluster in the center with $E(h) = E(p_{12}) = \frac{1}{2}$. Panel (b) shows slices through this fitness surface, demonstrating that the selection on heterozygosity, p_{12}, will differ according to cross type. For the F2 (F1×F1), heterozygosity is under directional selection, towards higher values. For backcrosses (such as BC1: F1×P1), then if the parental types are well adapted, heterozygosity is under symmetrical diversifying selection, away from the Mendelian expectation for the first backcross, and towards higher or lower values.

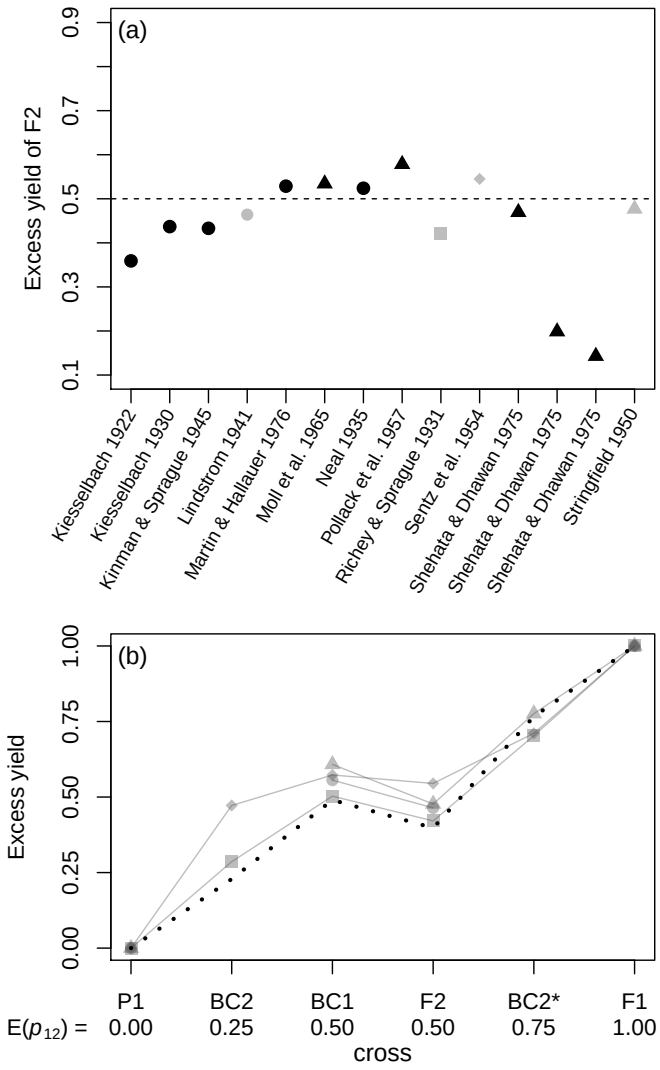

Figure 3: Data on hybrid vigor, from crosses of inbred *Zea mays*. The original data were collated by Wright (1977; see his Table 2.3.2), and Hallauer et al. (2010; see their Table 9.13), including only data from single crosses, where there was hybrid vigor in the F2, and yield was measured in quintals per hectare. Panel (a) plots the excess yield of the F2 (eq. 17). Results are shown for variety crosses (black triangles), as well as crosses of inbred lines in the strict sense (all other points). The dashed line shows the prediction of 0.5 from single-locus theory (eq. 18). Panel (b) shows the four data sets collated by Wright (1977), which allow us to compare the F2 and various backcrosses. These crosses, chosen to yield different levels of heterozygosity, are the parental type (P1), the second backcross (BC2 $= (\text{F1} \times \text{P1}) \times \text{P1}$); the first backcross (BC1 $= \text{F1} \times \text{P1}$), the F2 (F1 $\times$ F1), second backcross to the other parent ($\text{BC2}* = (\text{F1} \times \text{P1}) \times \text{P2}$), and the F1 (P1 $\times$ P2) (The data of Stringfield 1950 replace BC2* with an F2 between two distinct F1, involving 3 distinct strains, but the predictions are unchanged). The grey symbols for the four data sets correspond to those used in panel (a). The dotted line in panel (b) shows predictions from Fisher's model, assuming that the between-strain divergence contains limited coadaptation. The prediction uses eqs. 19-20 and 17, with $f_{\text{P}} = 0.75$, and $\beta = 2.5$, which was chosen to fit the data of Richey and G. F. Sprague (1931). The model predicts both the roughly linear increase in vigor with heterozygosity, and the systematic difference between BC1 and F2.

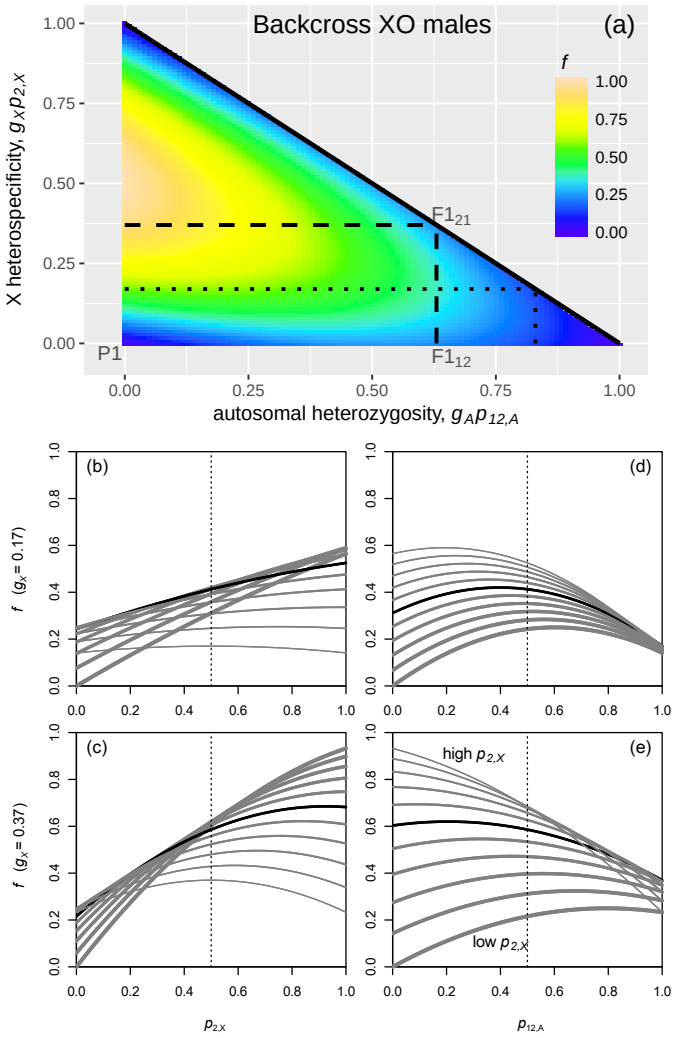

Figure 4: Predictions of Fisher's geometric model for heterogametic male hybrids. For simplicity, the predictions neglect any contributions from uniparentally-inherited loci, and assume that the parental types are well adapted. For concreteness, we assume XO sex determination, so that hybrids differ in their autosomal heterozygosity, $p_{12,A}$ and the proportion of alleles on the X that are heterospecific, $p_{2,X}$. Panel (a) shows the fitness surface as a function of these two quantities. The dotted lines delimit the region that would apply to a species pair with $g_X = 0.17$ (as we have estimated for *Drosophila simulans/sechellia* and *D. santomea/yakuba*), and the dashed lines delimit the region that would apply to a species pair with $g_X = 0.37$ (as we have estimated for *Drosophila persimilis/pseudoobscura*). Panels (b)-(e) show slices through this fitness surface, with vertical dotted lines showing the Mendelian expectations for a first backcross. Panels (b) and (c) show the dependency on X-linked heterospecificity. Results are shown when the autosomal heterozygosity is equal to its Mendelian expectation of $E(p_{12,A}) = \frac{1}{2}$ (black line), and over a range of values from $p_{12,A} = 0$ (thickest gray line) to $p_{12,A} = 1$ (thinnest gray line). Similarly, panels (d) and (e) show the dependency on autosomal heterozygosity, when the X-linked heterospecificity is at its expected value of $E(p_{2,X}) = \frac{1}{2}$ (black line), or over a range of values from $p_{2,X} = 0$ (thickest gray line) to $p_{2,X} = 1$ (thinnest gray line). Together, the plots show that Fisher's geometric model can account for the surprising results of Moehring (2011), and generate a new supported prediction (Table 3).

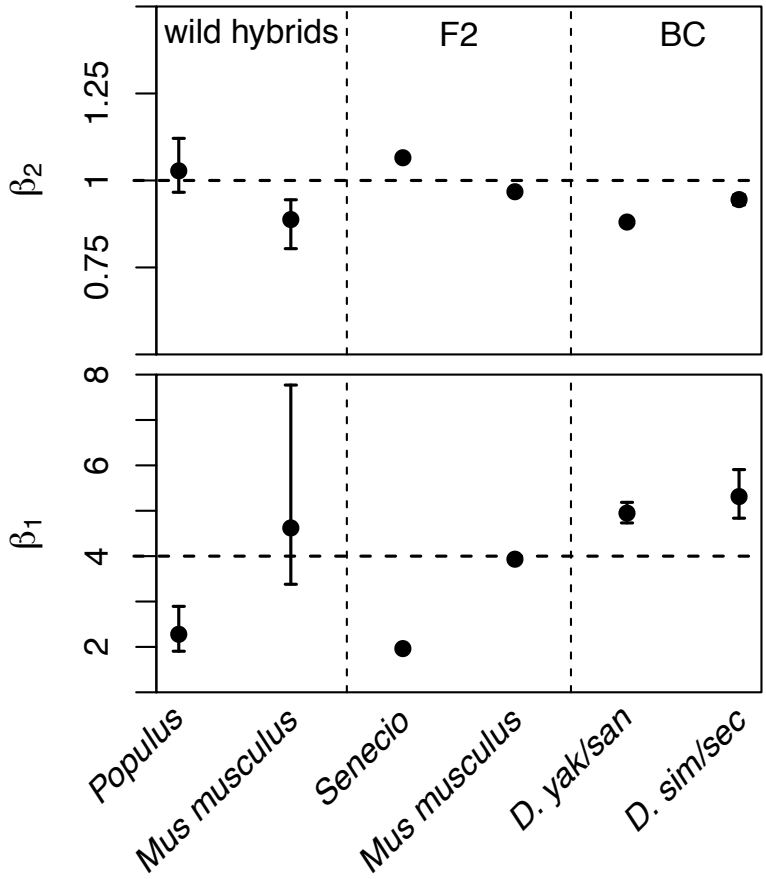

Figure 5: Best fit parameter estimates for the GLM of eq. 29, fit to fitness and genomic data from six data sets of hybrids (see Table 1 for details). The upper panel shows estimates of the coefficient β_2 which determines the form of selection acting on the hybrid index, h. Estimates of $\beta_2 = 1$ are consistent with symmetrical diversifying selection. The lower panel show estimates of the coefficient β_1 which determine the relative strength of selection acting on the hybrid index. Estimates of $\beta_1 = 4$ are predicted when the parental types are well adapted (eq. 7), while estimates $0 < \beta_1 < 4$ are predicted when the parental types are maladapted (eq. 9). Confidence intervals are defined as values that reduce the AIC by 2 units. These measures of uncertainty were not obtained for the F2 data, where variation in the hybrid index contributed little to the model fit, as predicted by eq. 19. Full details of the model fitting are found in the Methods and Supplementary Tables S2 and S3.

Table 1: Data sets

	Hybridization	N	Sex	#Markers	Cross	g_X	Fitness measure	Reference
Zea mays	inbred lines	-	☿	-	Various	-	Excess yield	See Fig. 3
Mytilus	*edulis/galloprovincialis*	132	♂/♀	43	F2	-	-	This study
		144	♂/♀	43	BC1	-	-	
Drosophila	*sechellia/simulans*	200/200	♂	8 X; 31 A	BC1	0.17	Sperm quantity: 3-pt. scale	Macdonald and Goldstein 1999
Drosophila	*santomea/yakuba*	550/549	♂	10 X; 22 A	BC1	0.17	Motile sperm: 9-pt. scale	Moehring et al. 2006a,b
Drosophila	*pseudoobscura/persimilis*	1141/1036	♂	2 X; 11 A	BC1	0.37	Motile sperm: present/absent	Noor et al. 2001
Teleogryllus	*oceanicus/commodus*	79	♀	-	BC1	0.30	Egg and offspring number	Moran et al. 2017
		108	♀	-	BC2	0.30	Egg and offspring number	
Populus	*alba/tremula*	137	♂/♀	~12,000	WH	-	Survival after 4 years	Christe et al. 2016
Senecio	*aethnensis/chrysanthemifolius*	64	☿	966	F2	-	Necrotic/Healthy	Chapman et al. 2016
Mus musculus	*musculus/domesticus*	185	♂	14,220	WH	0.039	Testes weight	Turner and Harr 2014
		305	♂	202 (16 X; 182 A)	F2	0.039	Prop. abnormal sperm	White et al. 2011

N: The number of individual hybrids, divided by backcross direction where appropriate; #Markers: The number of genetic markers used to estimate p_{12} and sometimes divided into X-linked and Autosomal. BC1: First backcross; BC2: Second backcross; WH: Wild hybrids. g_X: weight given to X-linked markers in the calculation of overall genome composition, calculated from the length of total annotated coding sequence.

Table 2: Tests for selection on heterozygosity in F2 and Backcrosses of *Mytilus* mussels.

Markers:	43	43	33	33
Data set:	All	No missing data	No missing data	Subsampled
Cross	$\hat{p}_{12}$ (N) p-value	$\hat{p}_{12}$ (N) p-value	$\hat{p}_{12}$ (N) p-value	$\hat{p}_{12}$ (N) p-value
F2	0.57 (132) 1.5×10^{-6}***	0.56 (88) 6.4×10^{-4}***	0.55 (91) 0.0033**	0.56 (56) 0.0020**
BC	0.57 (144) 1.3×10^{-4}***	0.53 (94) 0.0282*	0.53 (105) 0.0569	0.52 (56) 0.5815

$\hat{p}_{12}$: the estimated median heterozyosity; N: the number of hybrid individuals sampled; p-value: result of a Wilcoxon test of the null hypothesis median $p_{12} = 0$; F2: random mating of F1 between *M. galloprovincialis* and *M. edulis*; BC: Backcross of the F1 to *M. galloprovincialis*. No missing data: all individuals with missing data for any of the markers were excluded; Subsampled: for the BC, any individual carrying a marker that was homozygous for the major allele carried by wild *M. edulis* populations was excluded; for the F2, we downsampled by sequencing order to equalize sample sizes.

Table 3: Regressions of male sterility on autosomal heterospecificity in *Drosophila* backcrosses

Backcross to	N	Model	Best-fit coefficients for $p_{12,A}$	AIC
D. pseudoobscura	582	two intercepts	-	601.31
		two intercepts + single slope	2.147	580.41
		two intercepts + two slopes	3.746 (low $p_{2,X}$); -1.973 (high $p_{2,X}$)	**558.91**
D. persimilis	610	two intercepts	-	603.53
		two intercepts + single slope	3.620	558.18
		two intercepts + two slopes	4.505 (low $p_{2,X}$); -1.876 (high $p_{2,X}$)	**545.87**

AIC: Akaike Information Criterion; preferred model shown in bold.

References

Abbott, R. J. and A. C. Brennan (2014). "Altitudinal Gradients, Plant Hybrid Zones and Evolutionary Novelty". *Phil. Trans. R. Soc. B Biol Sci.* 369.1648. DOI: 10.1098/rstb.2013.0346.

Abbott, R. J. et al. (2013). "Hybridization and Speciation". *Journal of Evolutionary Biology* 26.2, pp. 229–246. DOI: 10.1111/j.1420-9101.2012.02599.x.

Agresti, A. (2003). *Categorical Data Analysis; Second Edition*. Hoboken, New Jersey: John Wiley & Sons, Inc.

Baird, S. J. E. (2017). "The Impact of High-Throughput Sequencing Technology on Speciation Research: Maintaining Perspective". *Journal of Evolutionary Biology* 30.8, pp. 1482–1487. DOI: 10.1111/jeb.13099.

Barton, N. H. (2001). "The Role of Hybridization in Evolution". *Molecular Ecology* 10.3, pp. 551–568. DOI: 10.1046/j.1365-294X.2001.01216.x.

Barton, N. H. (2017). "How Does Epistasis Influence the Response to Selection?" *Heredity* 118.1, pp. 96–109. DOI: 10.1038/hdy.2016.109.

Bierne, N., F. Bonhomme, P. Boudry, M. Szulkin, and P. David (2006). "Fitness Landscapes Support the Dominance Theory of Post-Zygotic Isolation in the Mussels *Mytilus Edulis* and *M. Galloprovincialis*." *Proc. R. Soc. B* 273.1591, pp. 1253–1260. DOI: 10.1098/rspb.2005.3440.

Bierne, N., P. David, P. Boudry, and F. Bonhomme (2002). "Assortative Fertilization and Selection at Larval Stage in the Mussels *Mytilus Edulis* and *M. Galloprovincialis*". *Evolution* 56.2, pp. 292–298. DOI: 10.1554/0014-3820(2002)056[0292:AFASAL]2.0.CO;2.

Boyle, E. A., Y. I. Li, and J. K. Pritchard (2017). "An Expanded View of Complex Traits: From Polygenic to Omnigenic". *Cell* 169.7, pp. 1177–1186. DOI: 10.1016/j.cell.2017.05.038.

Buerkle, C. A. (2017). "Inconvenient Truths in Population and Speciation Genetics Point towards a Future beyond Allele Frequencies". *Journal of Evolutionary Biology* 30.8, pp. 1498–1500. DOI: 10.1111/jeb.13106.

Caseys, C., C. Stritt, G. Glauser, T. Blanchard, and C. Lexer (2015). "Effects of Hybridization and Evolutionary Constraints on Secondary Metabolites: The Genetic Architecture of Phenylpropanoids in European Populus Species". *PLoS ONE* 10.5, e0128200. DOI: 10.1371/journal.pone.0128200.

Chapman, M. A., S. J. Hiscock, and D. A. Filatov (2016). "The Genomic Bases of Morphological Divergence and Reproductive Isolation Driven by Ecological Speciation in *Senecio* (Asteraceae)". *Journal of Evolutionary Biology* 29.1, pp. 98–113. DOI: 10.1111/jeb.12765.

Chevin, L.-M., G. Decorzent, and T. Lenormand (2014). "Niche Dimensionality and the Genetics of Ecological Speciation". *Evolution* 68.5, pp. 1244–1256. DOI: 10.1111/evo.12346.

Christe, C., K. N. Stölting, L. Bresadola, B. Fussi, B. Heinze, D. Wegmann, and C. Lexer (2016). "Selection against Recombinant Hybrids Maintains Reproductive Isolation in Hybridizing *Populus* Species despite F_1 Fertility and Recurrent Gene Flow". *Molecular Ecology* 25.11, pp. 2482–2498. DOI: 10.1111/mec.13587.

Coyne, J. A. and H. A. Orr (1989). "Two Rules of Speciation". *Speciation and Its Consequences*. D. Otte and J. A. Endler. Sinauer Associates, pp. 180–207.

Coyne, J. A. and H. A. Orr (2004). *Speciation*. Vol. 37. Sinauer Associates Sunderland, MA.

Crow, J. F. (1952). "Dominance and Overdominance". *Heterosis*. J. W. Gowen. Iowa State College Press.

Davis, A. W. and C.-I. Wu (1996). "The Broom of the Sorcerer's Apprentice: The Fine Structure of a Chromosomal Region Causing Reproductive Isolation Between Two Sibling Species of *Drosophila*". *Genetics* 143.3, pp. 1287–1298.

Demuth, J. P. and M. J. Wade (2005). "On the Theoretical and Empirical Framework for Studying Genetic Interactions within and among Species." *The American Naturalist* 165.5, pp. 524–536. DOI: 10.1086/429276.

Dobzhansky, T. G. (1937). *Genetics and the Origin of Species*. New York, NY: Columbia university press.

Duranton, M., F. Allal, C. Fraïsse, N. Bierne, F. Bonhomme, and P.-A. Gagnaire (2017). "The Origin and Remolding of Genomic Islands of Differentiation in the European Sea Bass". *bioRxiv*. DOI: 10.1101/223750.

Edmands, S. (2002). "Does Parental Divergence Predict Reproductive Compatibility?" *Trends in Ecology & Evolution* 17.11, pp. 520–527.

Fisher, R. A. (1930). *The Genetical Theory of Natural Selection*. Oxford, UK: Clarendon Press.

Fitzpatrick, B. M. (2008). "Hybrid Dysfunction: Population Genetic and Quantitative Genetic Perspectives". *The American Naturalist* 171.4, pp. 491–498. DOI: https://doi.org/10.1086/528991.

Fitzpatrick, B. M. (2012). "Estimating Ancestry and Heterozygosity of Hybrids Using Molecular Markers". *BMC Evolutionary Biology* 12.1, p. 131. DOI: 10.1186/1471-2148-12-131.

Fraïsse, C., J. A. D. Elderfield, and J. J. Welch (2014). "The Genetics of Speciation: Are Complex Incompatibilities Easier to Evolve?" *Journal of Evolutionary Biology* 27.4, pp. 688–699. DOI: 10.1111/jeb.12339.

Fraïsse, C., K. Belkhir, J. J. Welch, and N. Bierne (2016a). "Local Interspecies Introgression Is the Main Cause of Extreme Levels of Intraspecific Differentiation in Mussels". *Molecular Ecology* 25.1, pp. 269–286. DOI: 10.1111/mec.13299.

Fraïsse, C., P. A. Gunnarsson, D. Roze, N. Bierne, and J. J. Welch (2016b). "The Genetics of Speciation: Insights from Fisher's Geometric Model". *Evolution* 70.7, pp. 1450–1464. DOI: 10.1111/evo.12968.

Gavrilets, S. (2004). *Fitness Landscapes and the Origin of Species*. Princeton, NJ: Princeton Univ. Press.

Gramates, L. S. et al. (2017). "FlyBase at 25: Looking to the Future". *Nucleic Acids Research* 45.D1, pp. D663–D671. DOI: 10.1093/nar/gkw1016.

Guerrero, R. F., C. D. Muir, S. Josway, and L. C. Moyle (2017). "Pervasive Antagonistic Interactions among Hybrid Incompatibility Loci". *PLoS Genetics* 13.6, e1006817. DOI: 10.1371/journal.pgen.1006817.

Haldane, J. B. S. (1922). "Sex Ratio and Unisexual Sterility in Hybrid Animals". *Journal of Genetics* 12.2, pp. 101–109. DOI: 10.1007/BF02983075.

Hallauer, A. R., M. J. Carena, and J. B. Mirandad Filho (2010). *Quantitative Genetics in Maize Breeding*. Vol. 6. Handbook of Plant Breeding. New York, NY: Springer.

Hinze, L. L. and K. R. Lamkey (2003). "Absence of Epistasis for Grain Yield in Elite Maize Hybrids". *Crop Science* 43.1, pp. 46–56. DOI: 10.2135/cropsci2003.4600.

Hogan, T. W. and P. G. Fontana (1973). "Restoration of Meiotic Stability Following Artificial Hybridisation and Selection in *Teleogryllus* (Orth., Gryllidae)". *Bulletin of Entomological Research* 62.4, pp. 557–563. DOI: 10.1017/S0007485300005459.

Hwang, S., S.-C. Park, and J. Krug (2017). "Genotypic Complexity of Fisher's Geometric Model". *Genetics* 206.2, pp. 1049–1079. DOI: 10.1534/genetics.116.199497.

Kalirad, A. and R. B. R. Azevedo (2017). "Spiraling Complexity: A Test of the Snowball Effect in a Computational Model of RNA Folding". *Genetics* 206, pp. 377–388. DOI: 10.1534/genetics.116.196030.

Kiesselbach, T. (1930). "The Use of Advanced Generation Hybrids as Parents of Double-Cross Seed Corn." *Journal of the American Society of Agronomy* 22, pp. 614–25.

Kiesselbach, T. A. (1922). "Corn Investigations". *Nebraska Agric. Exp. Stn. Bull.* 20, pp. 5–151.

Kinman, M. L. and G. Sprague (1945). "Relation between Number of Parental Lines and Theoretical Performance of Synthetic Varieties of Corn". *Journal of the American Society of Agronomy* 37, pp. 341–351.

Li, X., X. Wang, Y. Wei, and E. C. Brummer (2011). "Prevalence of Segregation Distortion in Diploid Alfalfa and Its Implications for Genetics and Breeding Applications". *Theoretical and Applied Genetics* 123.4, pp. 667–679. DOI: 10.1007/s00122-011-1617-5.

Lindstrom, E. W. (1941). "Analysis of Modern Maize Breeding Principles and Methods". *Proc. 7th Intl. Genet. Congress*, pp. 151–156.

Lindtke, D., C. A. Buerkle, T. Barbará, B. Heinze, S. Castiglione, D. Bartha, and C. Lexer (2012). "Recombinant Hybrids Retain Heterozygosity at Many Loci: New Insights into the Genomics of Reproductive Isolation in *Populus*". *Molecular Ecology* 21.20, pp. 5042–5058. DOI: 10.1111/j.1365-294X.2012.05744.x.

Lindtke, D., Z. Gompert, C. Lexer, and C. A. Buerkle (2014). "Unexpected Ancestry of *Populus* Seedlings from a Hybrid Zone Implies a Large Role for Postzygotic Selection in the Maintenance of Species". *Molecular Ecology* 23.17, pp. 4316–4330. DOI: 10.1111/mec.12759.

Lynch, M. (1991). "The Genetic Interpretation of Inbreeding Depression and Outbreeding Depression". *Evolution* 45.3, pp. 622–629.

Macdonald, S. J. and D. B. Goldstein (1999). "A Quantitative Genetic Analysis of Male Sexual Traits Distinguishing the Sibling Species *Drosophila Simulans* and *D. Sechellia*". *Genetics* 153.4, pp. 1683–1699.

Mank, J. E., D. J. Hosken, and N. Wedell (2011). "Some Inconvenient Truths about Sex Chromosome Dosage Compensation and the Potential Role of Sexual Conflict". *Evolution* 65.8, pp. 2133–2144.

Manna, F., G. Martin, and T. Lenormand (2011). "Fitness Landscapes: An Alternative Theory for the Dominance of Mutation". *Genetics* 189.3, pp. 923–937. DOI: 10.1534/genetics.111.132944.

Martin, G. (2014). "Fisher's Geometrical Model Emerges as a Property of Complex Integrated Phenotypic Networks". *Genetics* 197.1, pp. 237–255. DOI: 10.1534/genetics.113.160325.

Martin, G. and T. Lenormand (2006). "A General Multivariate Extension of Fisher's Geometrical Model and the Distribution of Mutation Fitness Effects Across Species". *Evolution* 60.5, pp. 893–907. DOI: 10.1554/05-412.1.

Martin, J. M. and A. R. Hallauer (1976). "Relation between Heterozygosis and Yield for Four Types of Maize Inbred Lines". *Egyptian J. Genet. Cytol* 5, pp. 119–135.

Maside, X. R. and H. F. Naveira (1996). "On the Difficulties of Discriminating between Major and Minor Hybrid Male Sterility Factors in *Drosophila* by Examining the Segregation Ratio of Sterile and Fertile Sons in Backcrossing Experiments". *Heredity* 77.4, pp. 433–438.

McFadden, D. (1974). "Conditional Logit Analysis of Qualitative Choice Behavior". *Frontiers in Econometrics*. P. Zarembka. OCLC: 673267. New York: Academic Press, pp. 105–142.

Melchinger, A. E. (1987). "Expectation of Means and Variances of Testcrosses Produced from F2 and Backcross Individuals and Their Selfed Progenies". *Heredity* 59.1, pp. 105–115.

Mendez, F., J. Watkins, and M. Hammer (2012). "A Haplotype at STAT2 Introgressed from Neanderthals and Serves as a Candidate of Positive Selection in Papua New Guinea". *The American Journal of Human Genetics* 91.2, pp. 265–274. DOI: 10.1016/j.ajhg.2012.06.015.

Moehring, A. J., A. Llopart, S. Elwyn, J. A. Coyne, and T. F. C. Mackay (2006a). "The Genetic Basis of Postzygotic Reproductive Isolation Between *Drosophila Santomea* and *D. Yakuba* Due to Hybrid Male Sterility". *Genetics* 173.1, pp. 225–233. DOI: 10.1534/genetics.105.052985.

— (2006b). "The Genetic Basis of Prezygotic Reproductive Isolation Between *Drosophila Santomea* and *D. Yakuba* Due to Mating Preference". *Genetics* 173.1, pp. 215–223. DOI: 10.1534/genetics.105.052993.

Moehring, A. J. (2011). "Heterozygosity and Its Unexpected Correlations with Hybrid Sterility". *Evolution* 65.9, pp. 2621–2630. DOI: 10.1111/j.1558-5646.2011.01325.x.

Moll, R. H., J. H. Lonnquist, J. V. Fortuno, and E. C. Johnson (1965). "The Relationship of Heterosis and Genetic Divergence in Maize". *Genetics* 52.1, pp. 139–144.

Moran, P. A., M. G. Ritchie, and N. W. Bailey (2017). "A Rare Exception to Haldanes Rule: Are X Chromosomes Key to Hybrid Incompatibilities?" *Heredity* 118.6, pp. 554–562.

Morán, T. and A. Fontdevila (2014). "Genome-Wide Dissection of Hybrid Sterility in Drosophila Confirms a Polygenic Threshold Architecture". *Journal of Heredity* 105.3, pp. 381–396. DOI: 10.1093/jhered/esu003.

Neal, N. P. (1935). "Decrease in Yielding Capacity in Advanced Generations of Hybrid Corn". *Journal of the American Society of Agronomy* 51, pp. 666–670.

Noor, M. A. F., K. L. Grams, L. A. Bertucci, Y. Almendarez, J. Reiland, and K. R. Smith (2001). "The Genetics of Reproductive Isolation and the Potential for Gene Exchange between *Drosophila Pseudoobscura* and *D. Persimilis* via Backcross Hybrid Males". *Evolution* 55.3, pp. 512–521. DOI: 10.1554/0014-3820(2001)055[0512:TGORIA]2.0.CO;2.

Orgogozo, V., K. W. Broman, and D. L. Stern (2006). "High-Resolution Quantitative Trait Locus Mapping Reveals Sign Epistasis Controlling Ovariole Number Between Two *Drosophila* Species". *Genetics* 173.1, pp. 197–205. DOI: 10.1534/genetics.105.054098.

Orr, H. A. (1995). "The Population Genetics of Speciation: The Evolution of Hybrid Incompatibilities". *Genetics* 139.4, pp. 1805–1813. DOI: 10.1534/genetics.107.081810.

Orr, H. A. (1998). "The Population Genetics of Adaptation: The Distribution of Factors Fixed during Adaptive Evolution". *Evolution* 52.4, pp. 935–949.

Pollak, E., H. F. Robinson, and R. E. Comstock (1957). "Inter-Population Hybrids in Open-Pollinated Varieties of Maize". *The American Naturalist* 91.861, pp. 387–391. DOI: 10.1086/282003.

Quinlan, A. R. and I. M. Hall (2010). "BEDTools: A Flexible Suite of Utilities for Comparing Genomic Features". *Bioinformatics* 26.6, pp. 841–842. DOI: 10.1093/bioinformatics/btq033.

R Core Team (2016). "R: A Language and Environment for Statistical Computing". *R Foundation for Statistical Computing, Vienna, Austria. URL https://www.R-project.org*.

Richey, F. D. and G. F. Sprague (1931). *Experiments on Hybrid Vigor and Convergent Improvement in Corn*. Tech. rep. 267. Washington D. C.: U.S. Department of Agriculture, pp. 1–22.

Rockman, M. V. (2012). "The QTN Program and the Alleles That Matter for Evolution: All That's Gold Does Not Glitter". *Evolution* 66.1, pp. 1–17. DOI: 10.1111/j.1558-5646.2011.01486.x.

Routtu, J. et al. (2014). "An SNP-Based Second-Generation Genetic Map of Daphnia Magna and Its Application to QTL Analysis of Phenotypic Traits". *BMC Genomics* 15, p. 1033. DOI: 10.1186/1471-2164-15-1033.

Roux, C., C. Fraïsse, J. Romiguier, Y. Anciaux, N. Galtier, and N. Bierne (2016). "Shedding Light on the Grey Zone of Speciation along a Continuum of Genomic Divergence". *PLoS Biology* 14.12. Ed. by C. Moritz, e2000234. DOI: 10.1371/journal.pbio.2000234.

Schiffman, J. S. and P. L. Ralph (2017). "System Drift and Speciation". *bioRxiv*. DOI: 10.1101/231209.

Schumer, M., C. Xu, D. Powell, A. Durvasula, L. Skov, C. Holland, S. Sankararaman, P. Andolfatto, G. Rosenthal, and M. Przeworski (2017). "Natural Selection Interacts with the Local Recombination Rate to Shape the Evolution of Hybrid Genomes". *bioRxiv*, p. 212407.

Semagn, K., R. Babu, S. Hearne, and M. Olsen (2014). "Single Nucleotide Polymorphism Genotyping Using Kompetitive Allele Specific PCR (KASP): Overview of the Technology and Its Application in Crop Improvement". *Molecular Breeding* 33.1, pp. 1–14. DOI: 10.1007/s11032-013-9917-x.

Sentz, J. C., H. F. Robinson, and R. E. Comstock (1954). "Relation between Heterozygosis and Performance in Maize". *Agronomy Journal* 46.11, pp. 514–520.

Shehata, A. H. and N. L. Dhawan (1975). "Genetic Analysis of Grain Yield of Maize as Manifested in Diverse Varietal Populations and Their Crosses". *Egyptian J. Genet. Cytol* 4, pp. 90–116.

Stringfield, G. (1950). "Heterozygosis and Hybrid Vigor in Maize." *Agronomy journal* 42, pp. 45–112.

Tenaillon, O., O. K. Silander, J.-P. Uzan, and L. Chao (2007). "Quantifying Organismal Complexity Using a Population Genetic Approach". *PLoS ONE* 2.2, e217. DOI: 10.1371/journal.pone.0000217.

Turelli, M. and L. C. Moyle (2007). "Asymmetric Postmating Isolation: Darwin's Corollary to Haldane's Rule". *Genetics* 176.2, pp. 1059–1088. DOI: 10.1534/genetics.106.065979.

Turelli, M. and H. A. Orr (2000). "Dominance, Epistasis and the Genetics of Postzygotic Isolation". *Genetics* 154.4, p. 1663.

Turner, L. M. and B. Harr (2014). "Genome-Wide Mapping in a House Mouse Hybrid Zone Reveals Hybrid Sterility Loci and Dobzhansky-Muller Interactions". *Elife* 3, e02504. DOI: 10.7554/eLife.02504.

Waser, N. M. (1993). "Population Structure, Optimal Outbreeding and Assortative Mating in Angiosperms". *The Natural History of Inbreeding and Outbreeding: Theoretical and Empirical Perspectives*. N. W. Thornhill. Chicago: University of Chicago Press, pp. 173–199.

Waxman, D. and J. J. Welch (2005). "Fisher's Microscope and Haldane's Ellipse". *The American Naturalist* 166.4, pp. 447–457. DOI: 10.1086/444404.

Welch, J. J. (2004). "Accumulating Dobzhansky-Muller Incompatibilities: Reconciling Theory and Data". *Evolution* 58.6, pp. 1145–1156. DOI: 10.1111/j.0014-3820.2004.tb01695.x.

Welch, J. J. and D. Waxman (2003). "Modularity and the Cost of Complexity". *Evolution* 57.8, pp. 1723–1734. DOI: 10.1111/j.0014-3820.2003.tb00581.x.

White, M. A., B. Steffy, T. Wiltshire, and B. A. Payseur (2011). "Genetic Dissection of a Key Reproductive Barrier Between Nascent Species of House Mice". *Genetics* 189.1, pp. 289–304. DOI: 10.1534/genetics.111.129171.

Wright, S. (1922). "Coefficients of Inbreeding and Relationship". *The American Naturalist* 56.645, pp. 330–338. DOI: 10.1086/279872.

— (1977). "Inbreeding Depression and Heterosis: Plants". *Evolution and the Genetics of Populations, Volume 3: Experimental Results and Evolutionary Deductions*. Vol. 3. Univ. of Chicago Press.

Xu, M. and X. He (2011). "Genetic Incompatibility Dampens Hybrid Fertility More Than Hybrid Viability: Yeast as a Case Study". *PLoS ONE* 6.4, e18341. DOI: 10.1371/journal.pone.0018341.